Self-antigen–specific CD8+ T cell precursor frequency determines the quality of the antitumor immune response

Gabrielle A. Rizzuto,[1,3] Taha Merghoub,[1] Daniel Hirschhorn-Cymerman,[1] Cailian Liu,[1] Alexander M. Lesokhin,[1] Diana Sahawneh,[1] Hong Zhong,[1] Katherine S. Panageas,[2] Miguel-Angel Perales,[1] Grégoire Altan-Bonnet,[1,3] Jedd D. Wolchok,[1,3] and Alan N. Houghton[1,3]

[1]Departments of Medicine and Immunology, [2]Department of Biostatistics and Epidemiology, Memorial Sloan-Kettering Cancer Center, New York, NY 10065
[3]Weill School of Medicine of Cornell University, New York, NY 10065

A primary goal of cancer immunotherapy is to improve the naturally occurring, but weak, immune response to tumors. Ineffective responses to cancer vaccines may be caused, in part, by low numbers of self-reactive lymphocytes surviving negative selection. Here, we estimated the frequency of CD8+ T cells recognizing a self-antigen to be <0.0001% (~1 in 1 million CD8+ T cells), which is so low as to preclude a strong immune response in some mice. Supplementing this repertoire with naive antigen-specific cells increased vaccine-elicited tumor immunity and autoimmunity, but a threshold was reached whereby the transfer of increased numbers of antigen-specific cells impaired functional benefit, most likely because of intraclonal competition in the irradiated host. We show that cells primed at precursor frequencies below this competitive threshold proliferate more, acquire polyfunctionality, and eradicate tumors more effectively. This work demonstrates the functional relevance of CD8+ T cell precursor frequency to tumor immunity and autoimmunity. Transferring optimized numbers of naive tumor-specific T cells, followed by in vivo activation, is a new approach that can be applied to human cancer immunotherapy. Further, precursor frequency as an isolated variable can be exploited to augment efficacy of clinical vaccine strategies designed to activate any antigen-specific CD8+ T cells.

CORRESPONDENCE
Alan N. Houghton:
houghtoa@mskcc.org
OR
Jedd D. Wolchok:
wolchokj@mskcc.org

Abbreviation used: DLN, draining LN.

Over a century ago, Ehrlich realized that animals must avoid "horror autotoxicus" and prevent immune attack on self-tissues. This is accomplished, in part, by deletion of highly self-reactive clones. The current T cell development paradigm reasons that thymocytes recognizing self-peptide–MHC complexes with high affinity are programmed to die. Yet, T cells are positively selected because of their ability to recognize a diverse set of self-peptides bound to MHC complexes (1, 2) and weak-to-moderate affinity self-reactive T cells do escape negative selection (3). Some of these CD8+ and CD4+ T cells are capable of recognizing self-antigens expressed by tumors, including cancer-testes antigens, and differentiation antigens (4). Melanosomal membrane glycoproteins are a well-characterized family of differentiation antigens that are recognized by low-frequency CD8+ T cells of melanoma patients (5). In the mouse, this family includes gp100/pmel-17, a type I melanosomal membrane protein involved in the polymerization of melanin (6).

To generate a robust immune response against a self-protein, mechanisms of tolerance must be circumvented. Vaccination with altered forms of the antigen is an effective, widely studied method of overcoming peripheral tolerance (7–9). We have reported preclinical and clinical use of a plasmid delivery system that utilizes high pressure to drive cutaneous particle bombardment of DNA, leading to presentation

J.D. Wolchok and A.N. Houghton contributed equally to this paper.

The Rockefeller University Press $30.00
J. Exp. Med. Vol. 206 No. 4 849-866
www.jem.org/cgi/doi/10.1084/jem.20081382

The Journal of Experimental Medicine

of antigen by dendritic cells in skin draining LNs (DLNs) (10, 11). Active immunization of mice with plasmid encoding human gp100 (hgp100) generates a response composed of $CD8^+$ T cells that cross-react with an immunodominant epitope (amino acids 25–33) from the wild-type self-protein presented by $H\text{-}2D^b$ (10, 12). Although this strategy allows for the generation of low-level, detectable responses, the growth of established tumors is barely impeded. Indeed, active vaccination strategies alone, although considered safe, have yielded poor responses in clinical trials (13).

Recent work has shown that delivering antitumor vaccines while cells are undergoing lymphopenia-induced homeostatic expansion enhances $CD8^+$ T cell responses (14, 15). This augmentation is caused by the availability of homeostatic cytokines, removal of regulatory populations, increased self-peptide–MHC reactivity of homeostatically proliferating cells, and irradiation-induced release of danger signals (16–18). We designed a strategy to induce more potent tumor immunity that combines sublethal irradiation, adoptive transfer of naive splenocytes, and vaccination against gp100. This treatment is moderately effective at preventing melanoma growth in a prophylactic setting, but is much less potent when administered to a tumor-bearing mouse (unpublished data). Fortunately, the literature suggests many ways to improve this treatment, including but not limited to, addition of adjuvants, multi-epitope vaccination, and targeted removal of suppressor populations. Here, we chose to focus on a previously unexplored parameter: the frequency of self-antigen–specific $CD8^+$ T cells present at the time of in vivo priming.

How many of the ~20 million naive $CD8^+$ T cells in a mouse are specific for a particular epitope? The theoretical diversity of TCRs on mature T cells has been estimated at $\sim 10^{13}$ possibilities (19), but this may be an overestimate if documented constraints and biases on the generation of functional TCRs are considered. The study of individual clonotypes in the preimmune repertoire is made difficult because it requires the detection of small numbers of cells among millions. Nevertheless, immunologists have used indirect and direct methods to assess the preimmune repertoire for several well-studied foreign epitopes. Estimates range from 10 to 3,000 antigen-specific cells/antigen/mouse (20–26). To date, the lowest reported estimates for epitope-specific frequency is ~16 $CD4^+$ cells recognizing OVA and the highest is ~3,000 $CD8^+$ T cells that recognize gp_{33} from LCMV (21, 24).

Two recent reports demonstrate that natural differences in the size of three $CD4^+$ (21) and six $CD8^+$ foreign antigen–specific T cell populations (22) are important determinants of the magnitude of the effector and memory response. Further, it has been suggested that low $CD8^+$ T cell precursor frequency may partially account for patterns of immunodominance and explain why certain well-processed and presented foreign epitopes fail to elicit strong immune responses in the context of infection (27, 28). Mechanisms of central and peripheral deletion might be expected to leave the mouse with even fewer precursors specific for self-antigens (29), thus limiting the generation of robust antitumor responses. We hypothesized that the strength of the antitumor immune response was in part determined by the size of the tumor-specific precursor pool. Therefore, we sought to determine the endogenous frequency of $CD8^+$ T cells specific for a self-antigen, and to characterize the antitumor immune response generated from different T cell precursor frequencies.

Here, we present our studies combining vaccination with adoptively transferred, naive, gp100-specific $CD8^+$ T cells activated in vivo. We estimate the frequency of endogenous $CD8^+$ cells recognizing $gp100_{25\text{-}33}$ to be extremely low, <0.0001% of $CD8^+$ T cells, an implication of which is that some genetically identical animals do not mount strong, protective responses to vaccination. We demonstrate that supplementing the naive repertoire with $gp100_{25\text{-}33}$-specific cells increases vaccine-elicited tumor immunity. However, at very high input numbers, this benefit is negated because of intraclonal competition. These data show that $CD8^+$ T cell precursor frequency has a striking effect on clinically relevant disease. Our results demonstrate that precursor frequency can be manipulated to advantage, and must at least be considered in therapeutic strategies of adoptive immunotherapy.

RESULTS

Determination of self-antigen–specific $CD8^+$ T cell precursor frequency

We have previously shown that repeated vaccination of naive wild-type mice with plasmid DNA encoding mutated melanoma antigens elicits a low-frequency $CD8^+$ T cell response (<1% IFN-γ^+ of $CD8^+$) (8). We found that a preconditioning regimen of sublethal irradiation (600 cGy) and adoptive transfer of 30 million naive splenocytes 1 d before the first vaccination increases the $CD8^+$ T cell response and enhances protection from subsequent challenge with tumor (unpublished data). This treatment strategy generates responses that are readily detectable by flow cytometry, and because it is a clinically relevant model, it was chosen for use in the experiments presented here.

As central and peripheral tolerance mechanisms might be expected to leave animals with few functional precursors specific for self-antigens, we wanted to determine the exact preimmune frequency for $CD8^+$ T cells recognizing a melanoma antigen and evaluate how this impacted our melanoma treatment strategy.

To indirectly assess this number within the preimmune, naive $CD8^+$ population, we adopted a method first described by Blattman et al. (23) and used the pmel-1 TCR transgenic mouse (30). Pmel-1 mice express a $V\alpha1V\beta13$ $gp100_{25\text{-}33}$–reactive TCR transgene, and thus served as a source of transplantable $CD8^+$ tumor-antigen–specific cells used to estimate precursor frequency for the gp100 self-antigen. It was reasoned that an antigen-induced effector response would be equally composed of endogenous and transgenic cells when they were present at similar initial precursor frequencies (23, 26). As validation of this approach using our tumor therapy model of irradiation and adoptive transfer, we performed a titration experiment with OT1 $CD8^+$ T cells. Mice were treated with 600 cGy irradiation, followed by adoptive transfer of different

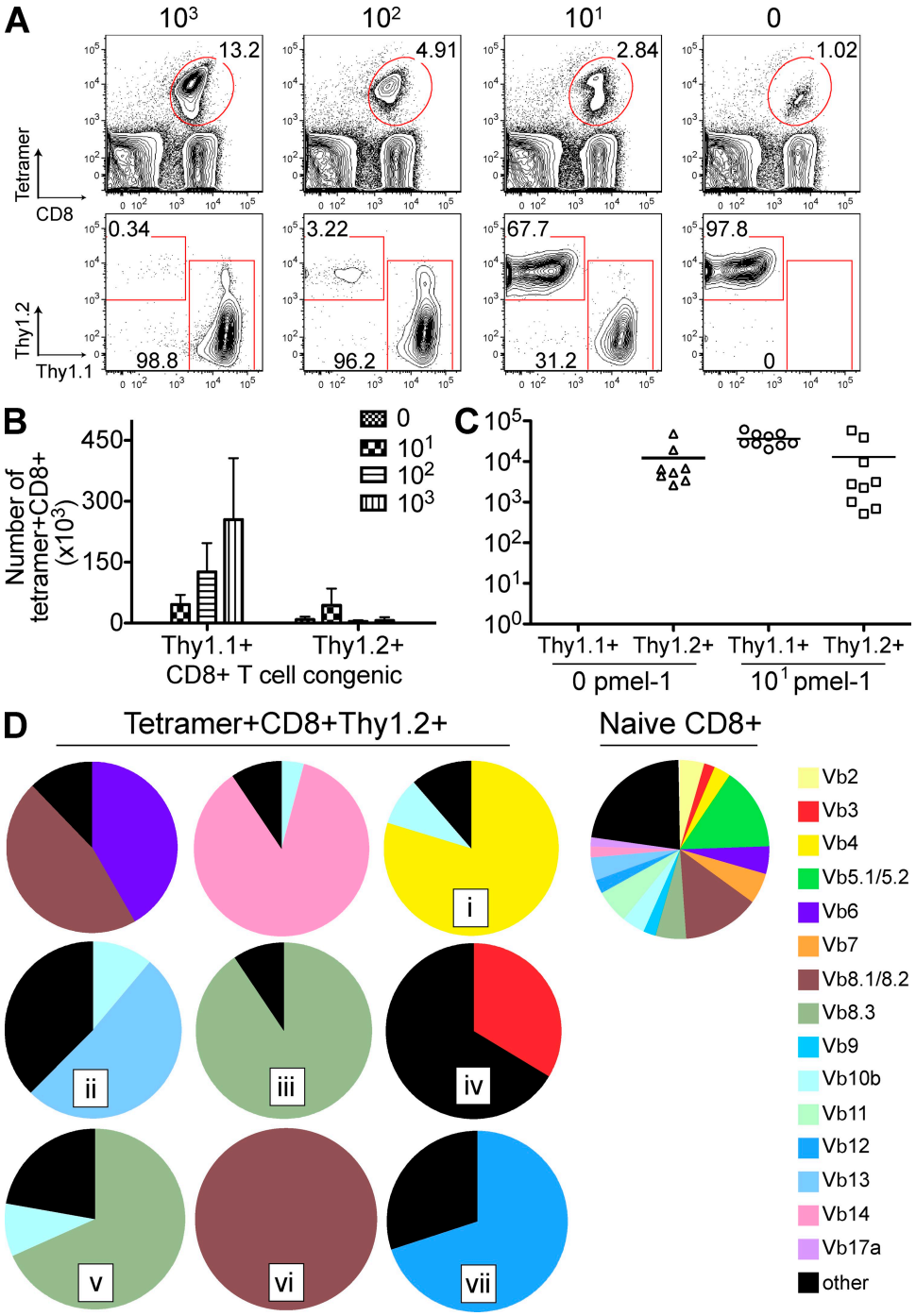

Figure 1. The precursor frequency of CD8⁺ T cells recognizing gp100$_{25-33}$ in the naive repertoire is estimated to be ~1 in 1 million CD8⁺ T cells; vaccination induces an oligoclonal, private response. (A and B) Sublethally irradiated animals received adoptive transfer with 30 million splenocytes containing titrating doses (0, 10^1, 10^2, and 10^3) of pmel-1 CD8⁺Thy1.1⁺ cells. Three weekly vaccinations with hgp100-encoding plasmid began the following day, and DLNs were harvested 5 d after the last vaccination. Cells were stained and analyzed by flow cytometry to determine frequency and absolute number of hgp100-tetramer⁺ cells, as well as the relative contributions of Thy1.1⁺ (transgenic) cells and Thy1.2⁺ (endogenous) to this response. In A, representative contour plots are shown for mice in each pmel-1 dose group. (B) Mean absolute number of CD8⁺tetramer⁺ cells in DLN (n = 3 mice/group; error bars represent the SD). (C) Larger cohorts (n = 10 mice/group) were prepared as in A, with animals receiving either 0 or 10^1 initial pmel-1 cells. The absolute number of Thy1.1⁺ (transgenic) or Thy1.2⁺ (endogenous) CD8⁺tetramer⁺ cells in DLNs of those animals that responded above background to vaccine is shown. Flow cytometric contour plots are displayed as supplemental data (Fig. S1). (D) Spleens and DLNs of responders were stained for TCR Vβ gene segment expression. Usage profiles for individual mice, as well as for CD8⁺ cells from a naive nonvaccinated control, are shown as pie graphs. Roman numerals indicate samples that were subjected to cloning of TCR Vβ CDR3 regions, as reported in Table I. Data shown in A–C are representative of at least three experiments performed under similar conditions. D is representative of nine individual mice from two independent experiments. Fig. S1 is available at http://www.jem.org/cgi/content/full/jem.20081382/DC1.

frequencies of OT1 $CD8^+$ T cells mixed with naive splenocytes. Because all mice receive the same total number of 30 million cells, the only variable is the frequency of transgenic cells. Vaccination with plasmid encoding SIINFEKL estimated OT1-specific precursor frequency to be between 10 and 100 cells (unpublished data). This is consistent with literature estimating the number of foreign antigen–specific $CD8^+$ cells within the naive repertoire (23, 31).

To measure $gp100_{25\text{-}33}$-specific endogenous precursor frequency, mice were sublethally irradiated and adoptively transferred with 30 million splenocytes that included 0, 10^1, 10^2, or 10^3 pmel-1 cells (Fig. 1). Starting the following day, animals were vaccinated weekly for 3 wk with plasmid encoding hgp100. 5 d after the last vaccination, individual spleens and DLNs were harvested, and the relative contributions of transgenic ($Thy1.1^+$) and endogenous ($Thy1.2^+$) cells to the gp100-$tetramer^+$ population was assessed (Fig. 1, A–C). The endogenous response was barely detectable in animals receiving 10^3 pmel-1 cells. This is most likely because 10^3 transgenic cells outcompete endogenous clones, suggesting an endogenous precursor frequency of <0.02%. The endogenous response was also largely eliminated when 10^2 pmel-1 cells were transferred (Fig. 1, A and B). However, mice receiving 10^1 pmel-1 cells generated a response that included endogenous cells (Fig. 1, A–C). Preparation of larger cohorts demonstrated that of 10 mice that received 0 pmel-1 cells, 2–3/10 mice had no detectable response above background (Fig. S1, available at http://www.jem.org/cgi/content/full/jem.20081382/DC1). One explanation for this is that these animals did not possess a TCR capable of recognizing this self-antigen at the time of vaccination. Finally, we comparatively assessed the affinity of endogenous and pmel-1 responders in individual mice. The frequency of IFN-γ^+ endogenous and/or pmel-1 cells were measured for titrating amounts of mouse $gp100_{25\text{-}33}$ peptide, and response curves were generated (unpublished data). When compared with pmel-1 cells, half-maximal recognition of $mgp100_{25\text{-}33}$ occurred at higher concentrations of peptide for endogenous responding cells. This suggests that these endogenous responders were of lower avidity than pmel-1 cells.

In this irradiation and adoptive transfer model, mice possessed $\sim 5 \times 10^6$ $CD8^+$ T cells at the time of first vaccination, therefore yielding a calculated precursor frequency of 1 $gp100_{25\text{-}33}$–specific cell per 1.0×10^6 $CD8^+$ T cells. This is approximately an order of magnitude lower than has been reported for $CD8^+$ T cells recognizing foreign antigens (22, 23, 31). Indeed, a precursor frequency of $\sim$5 $gp100_{25\text{-}33}$–specific cells/mouse would suggest that small numbers of clones are represented in the effector population. To directly test whether the endogenous hgp100-$tetramer^+$ population was oligoclonal, we stained cells from individual responders with antibodies recognizing TCR Vβ families. As shown in Fig. 1 D, each of nine individual responses tested was composed of between one and four Vβ families, with no evidence of a preferred Vβ. To address the number of clones present within each responding Vβ family, hgp100-$tetramer^+$ cells were FACS sorted, and TCR Vβ CDR3 regions were PCR amplified, cloned, and sequenced. Remarkably, nearly all of the individual Vβ families contained only one or two CDR3 regions (Table I).

These results reveal that the $CD8^+$ T cell response to the self-epitope $gp100_{25\text{-}33}$ is oligoclonal and private. The data suggest that in some genetically identical animals, the $gp100_{25\text{-}33}$–specific precursor frequency may reach "functional" zero. A similar low frequency of tumor-specific cells in cancer patients may contribute to poor responses to cancer vaccines targeting self-antigens, and provides rationale for supplementing the naive repertoire with increased numbers of antigen-specific $CD8^+$ T cells.

Initial self-antigen–specific $CD8^+$ precursor frequency dictates tumor immunity and autoimmunity in a therapeutic model

We sought to assess the role of tumor-specific $CD8^+$ cell precursor frequency in rejection of intradermal melanoma tumors and hypothesized that treatment efficacy would be

Table I. Summary of endogenous TCR Vβ and TCR Jβ segment usage and CDR3 sequences

Mouse	Percent positive for Vβ by flow cytometry	CDR3-IMGT	TRBV gene	TRBJ gene	Number of identical clones	GenBank accession no.
i	80% Vβ4	A S S Q S R Y E Q Y	2*01	2-7*01	18/19[a]	EU647570
	9% Vβ10b	A S S S S G F T E V F	4*01	1-1*01 or 02	14/15[b]	EU647566
ii	51% Vβ13	A S S F T Q T N T E V F	14*01	1-1*01	13/13	EU647568
	11% Vβ10b	A S S S T G Y Y A E Q F	4*01	2-1*01	18/18	EU647569
iii	91% Vβ8.3	A S R D G S Y N S P L Y	13-1*01 or 02	1-6*01	32/32	EU647565
iv	34% Vβ3	A S S L S T G Y Y A E Q F	26*01 or 02	2-1*01	20/20	EU647574
v	65% Vβ8.3	A S S E P T G G V Y E Q Y	13-1*01 or 02	2-7*01	17/17	EU647575
	9.5% Vβ10b	A S S S G G G Y A E Q F	4*01	2-1*01	11/11	EU647577
vi	100% Vβ8.1/8.2	A S G D A W A G S Y E Q Y	13-2*01 or 03, or 04	2-7*01	19/20[c]	EU647573
vii	70% Vβ12	A S S L A D R G Q D T Q Y	15*01	2-5*01	19/19	EU647576

[a]For 1/19 clones CDR3-IMGT is A S N Q S R Y E Q Y (accession no. EU647571).
[b]For 1/15 clones CDR3-IMGT is A S I R G T E V F (accession no. EU647567).
[c]For 1/20 clones CDR3-IMGT is A S G D P W A G S Y E Q Y (accession no. EU647572).

improved by supplementing the low-frequency $gp100_{25-33}$-specific repertoire with naive pmel-1 cells. As depicted in Fig. 2 A, mice bearing day 4 cutaneous B16 melanoma tumors were treated with 600 cGy, followed by adoptive transfer of different frequencies of pmel-1 cells mixed with naive splenocytes. This treatment model ensures that all mice receive the same total number of 30 million transferred cells; the variable is the frequency of pmel-1 cells. Dose groups ranged from physiological frequencies of <0.02% to supraphysiological levels orders of a magnitude higher (Fig. 2 A).

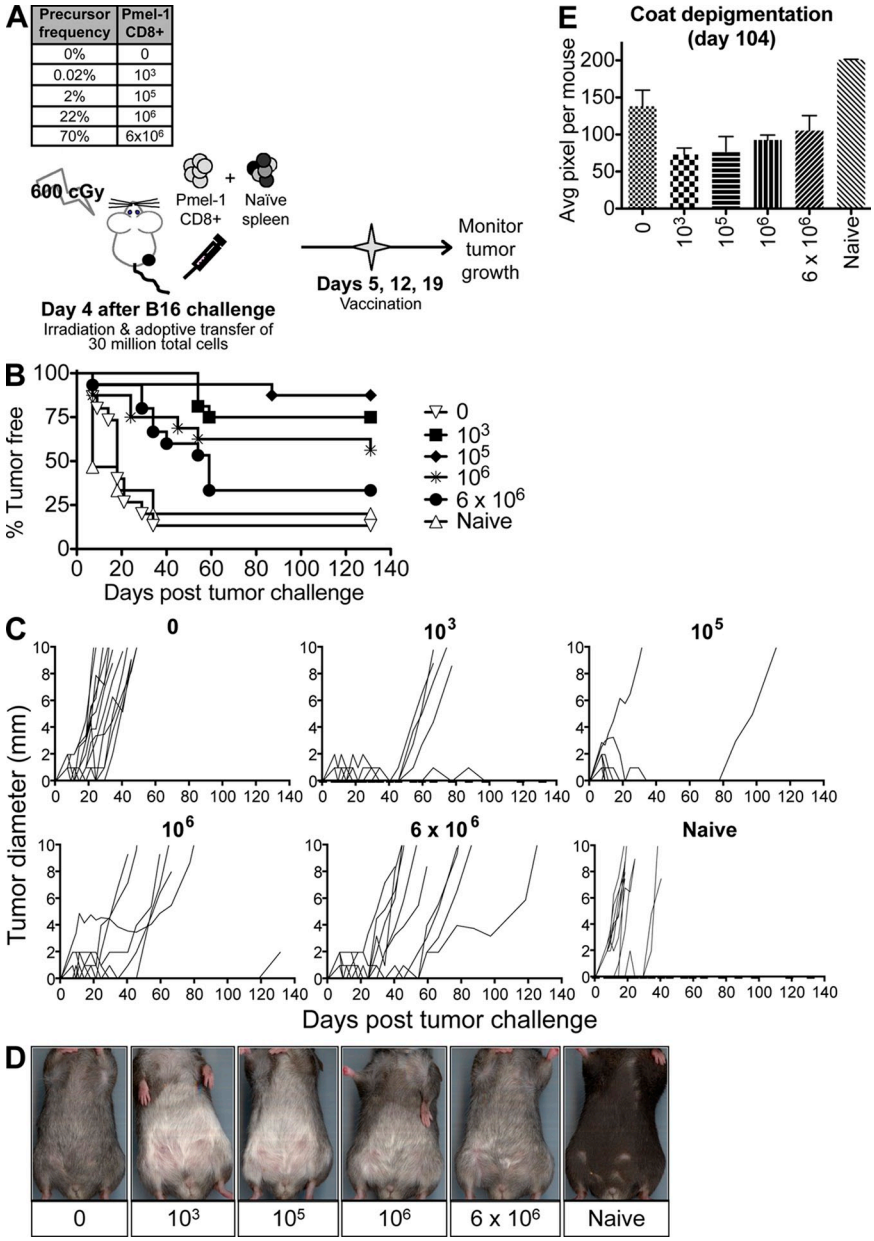

Figure 2. Tumor growth and autoimmune depigmentation elicited by adoptive transfer and vaccination is inversely correlated with CD8⁺ cell precursor frequency. (A) Experimental scheme. Thy1.2⁺ mice (15–16 mice/group) were intradermally inoculated with B16 cells and either left untreated (naive) or began treatment on day 4 consisting of sublethal irradiation and adoptive transfer of donor cells. Each experimental group received adoptive transfer of 30 million Thy1.1⁺ splenocytes, containing varying numbers of purified CD8⁺Thy1.1⁺ pmel-1 cells. All treated mice received three weekly vaccinations with hgp100-encoding plasmid, beginning on day 5. Animals were monitored every 3–5 d for tumor growth. (B) Incidence of progressively growing B16 tumors. (C) Tumor growth curves for individual mice. (D) At day 104 after tumor challenge, surviving mice were anaesthetized and imaged using a flatbed scanner. Representative ventral images from 1 animal/group are shown. Depigmentation was quantified, and mean pixel number and SEM is plotted in E. For groups receiving 10^3, 10^5, 10^6, and 6×10^6 pmel-1 cells, $P < 0.001$ for an overall association between the number of pixels and the initial pmel-1 dose. Pairwise comparisons for differences yield $P < 0.001$ for 10^3 versus 10^6 and $P < 0.01$ for 10^3 versus 6×10^6. Data are representative of two experiments.

Beginning the following day, these mice were vaccinated weekly for 3 wk with plasmid-encoding hgp100.

In this model, tumors in untreated animals become palpable at ~7 d (Fig. 2 C). Notably, lower initial pmel-1 precursor frequencies (0.02% and 2%) resulted in enhanced tumor rejection of these early progressing tumors. A delay in tumor progression was noticed at all pmel-1 doses, but tumor-free survival was most significantly enhanced at the 10^3 and 10^5 pmel-1 doses (Fig. 2, B and C). Adding no pmel-1 cells to the adoptive transfer is of similar efficacy to the 6×10^6 pmel-1 dose (Fig. 2 and Table II). The overall frequency of mice without tumors at experimental endpoints, and the statistical significance for two experiments, is reported in Table II.

Effective generation of immunity to B16 by vaccination with mutated self-antigen often results in autoimmunity (9). Although vaccination of naive wild-type mice with hgp100 is not a particularly strong inducer of autoimmune coat depigmentation, our treatment regimen did result in overt depigmentation, particularly in the low pmel-1 dose groups. Depigmentation was inversely correlated with pmel-1 dose for animals receiving pmel-1 cells. At day 104 after tumor challenge, coat depigmentation was quantified for surviving mice (Fig. 2 E). Representatives from each group are shown in Fig. 2 D.

These results identify vaccine-specific $CD8^+$ precursor frequency as a remarkably significant predictor of treatment and side-effect outcome. Paradoxically, above a certain threshold there is an inverse relationship between pmel-1 clonal frequency and vaccine-induced tumor rejection and autoimmune depigmentation. In contrast, studies using the transfer of in vitro–activated, tumor-specific cells have demonstrated that transfer of greater cell numbers is generally more effective (32). Therefore, we considered that at high precursory frequency, the in vivo activation of naive pmel-1 cells was compromised.

Increased fold expansion of pmel-1 cells is observed at lower precursor frequencies

We characterized the antitumor immune response generated from the different pmel-1 precursor frequencies. We began by measuring the expansion of pmel-1 cells that is expected to occur several days after initial antigen encounter. Mice were subcutaneously inoculated with B16 melanoma cells mixed in Matrigel, which is a commercially available extracellular matrix. This allowed for subsequent tumor removal at early days after treatment, and isolation and flow cytometric analysis of tumor infiltrating lymphocytes. On day 4 after tumor injection, mice underwent treatment consisting of sublethal irradiation, adoptive transfer with different pmel-1 cell precursor frequencies, and vaccination (Fig. 3 A).

At days 3, 6, 8, and 13 after irradiation and adoptive transfer, tumor, spleen and DLN were harvested and processed to determine cell number and frequency of pmel-1 cells by flow cytometry. Fold expansion was calculated by dividing $Thy1.1^+$ pmel-1 frequency in the $CD8^+$ population at each time point by initial pmel-1 frequency in the adoptively transferred $CD8^+$ population. The data for mean fold expansion (Fig. 3 B) reveals that during this first week, pmel-1 cells present at 0.02% initial precursor frequency underwent a remarkable 50–450-fold expansion. Over this same time period, pmel-1 cells present at 2% initial precursor frequency expanded approximately fivefold, whereas cells in the two higher dose groups barely maintained their input numbers. A similar trend was observed 5 d after the second vaccination (Fig. 3 B, Day 12), with marked increases in the fold expansion of the pmel-1 population notable only in the low-dose groups. Consistently, expression of the proliferation marker Ki67 in pmel-1 cells 5 d after the second vaccination was lower on cells primed at higher precursor frequencies (Fig. 3 C).

Thus, fewer pmel-1 cells transferred into a lymphopenic host resulted in greater expansion of the pmel-1 population in response to vaccine. The fact that this level of expansion is not observed in unvaccinated recipients (not depicted), suggests that detection of self-$gp100_{25–33}$ present in melanocytic tissue is not sufficient to drive robust expansion of pmel-1 cells. This is presumably caused by the reported lower affinity of these cells for the mouse epitope, such that it is incapable of priming a full proliferative response (30, 33).

At higher precursor frequencies, intraclonal competition impairs proliferation and acquisition of an activated effector phenotype

To test if the impaired expansion of pmel-1 cells at the higher doses is caused by intraclonal competition, we measured the proliferation of 10^5 pmel-1 cells in the presence of competing

Table II. Summary of percentage tumor-free mice at endpoint of experiment described in Fig. 2

Treatment group	Tumor-free /total mice replicate 1	Tumor-free /total mice replicate 2	Combined percent tumor free	Statistical significance		
				versus 6×10^6	versus 0	versus naive
10^3	11 / 14	12 / 16	77%	$P < 0.01$	$P < 0.001$[a]	$P < 0.001$[a]
10^5	11 / 15	14 / 16	81%	$P < 0.01$	$P < 0.001$[a]	$P < 0.001$[a]
10^6	10 / 15	9 / 16	52%		$P < 0.05$	$P < 0.001$[a]
6×10^6	5 / 12	5 / 15	37%			
0 (no pmel)	6 / 14	2 / 15	28%			
Naive	1 / 10	3 / 15	16%			

Endpoint was day 104 (replicate 1) and day 131 (replicate 2) post-tumor challenge. Statistical significance was calculated for combined experiment.
[a]Indicates values remaining significant after correction for multiple comparisons.

pmel-1 cells (Fig. 4 A). Sublethally irradiated recipients received adoptive transfer of naive splenocytes that included 10^5 CFSE-labeled pmel-1 cells. Co-transfer of unlabeled, double-positive Thy1.1$^+$Thy1.2$^+$ pmel-1 cells allowed for flow cytometric distinction of competitors from extensively proliferated Thy1.1$^+$ pmel-1 cells. We also included recipient animals that received competitor CD8$^+$ OT1 cells. This served to test if the moderately increased number of total CD8$^+$ cells transferred at the 6×10^6 pmel-1 dose was impairing proliferation irrespective of peptide-MHC specificity.

The extent of proliferation of Thy1.1$^+$ pmel-1 cells located in DLNs is shown in Fig. 4 B, and individual mouse variation is reported in Fig. 4 C. Thy1.1$^+$ pmel-1 cells in nonvaccinated controls underwent several rounds of proliferation, as is expected for CD8$^+$ T cells transferred into irradiated hosts (34). Vaccine greatly enhanced this proliferative burst, whereas addition of 0.9×10^6 pmel-1 competitors partially reversed this effect. Addition of 5.9×10^6 pmel-1 competitors more dramatically inhibited proliferation of the Thy1.1$^+$ pmel-1 cells. However, when 5.9×10^6 OT1 competitors were cotransferred, proliferation and activation of Thy1.1$^+$ pmel-1 cells was

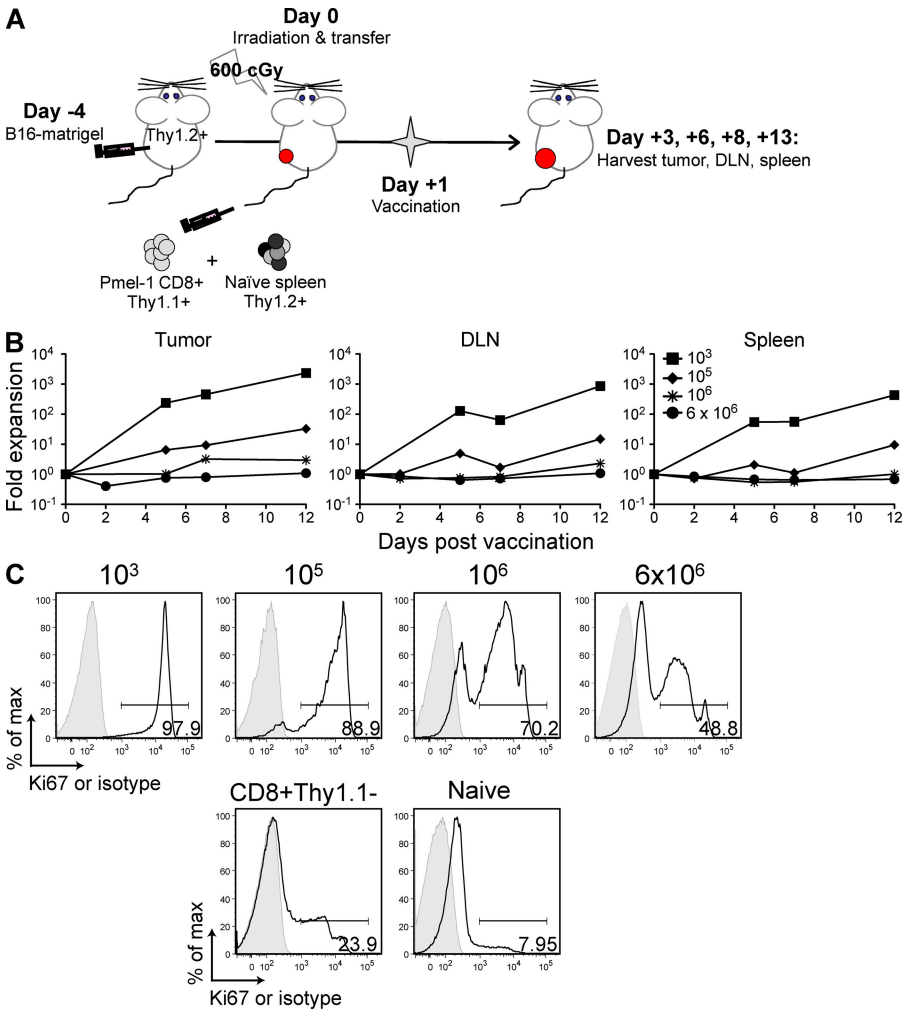

Figure 3. Higher pmel-1 fold expansion at lower initial precursor frequency. (A) Experimental scheme. Thy1.2$^+$ mice were challenged with a supra-lethal dose of B16-matrigel 4 d before treatment. Animals were treated with sublethal irradiation and adoptive transfer of 30 million Thy1.2$^+$ splenocytes, with groups (n = 6 mice/group) receiving different precursor frequencies of CD8$^+$Thy1.1$^+$ pmel-1 cells. One day later all were vaccinated with hgp100-encoding plasmid. (B) At time points shown, tumor, spleen, and DLN from two mice per group were harvested, and the frequency of pmel-1 CD8$^+$ cells was determined by flow cytometry. Fold expansion was calculated by dividing Thy1.1$^+$ pmel-1 frequency among all CD8$^+$ at each time point by initial frequency. The mean of two individual mice is shown. Representative of three individual experiments performed under similar conditions. (C) In separate experiments, nontumor-bearing animals were treated as described above with pmel-1 doses of 10^3, 10^5, 10^6, or 6×10^6 cells, vaccinated 1 d after adoptive transfer and 1 wk later. 5 d after the second vaccination, DLNs were harvested and stained for intracellular expression of Ki67. Flow cytometric overlaid histograms of Ki67 and isotype control (shaded) staining for the different pmel-1 dose groups are shown. Representative plots of nongp100-specific, CD8$^+$ cells (CD8$^+$Thy1.1$^-$) in the lymphopenic host, as well as naive CD8$^+$ cells are shown. Similar pattern of Ki67 reactivity observed in three individual experiments.

not affected (Fig. 4, B and C). This suggests that competition for hgp100$_{25-33}$–peptide–MHC complexes is occurring, and not as obviously for a non–TCR-specific signal, such as access to APCs or space in the DLNs. We considered that pmel-1 cells might also compete for endogenous peptide–MHC complexes, driving homeostatic expansion for that TCR clone. Therefore, we assessed homeostatic proliferation of pmel-1 cells in the lymphopenic host in the absence of vaccination. Higher pmel-1 cell doses resulted in slightly less vigorous homeostatic proliferation (unpublished data). The inhibition, however, was not as dramatic as was observed in the presence of vaccine-delivered antigen.

Pmel-1 cells that had productively encountered antigen would be expected to acquire an activated phenotype. Therefore, we looked at the activation state of the Thy1.1$^+$ pmel-1 cells. Addition of pmel-1, but not OT1, competitors resulted in lower frequencies of cells that up-regulated CD44 and down-regulated CD62L, which is consistent with an effector phenotype (CD44^{hi}CD62L^{lo}; Fig. 4, B and D, and not depicted). In related experiments, we tested the acquisition of

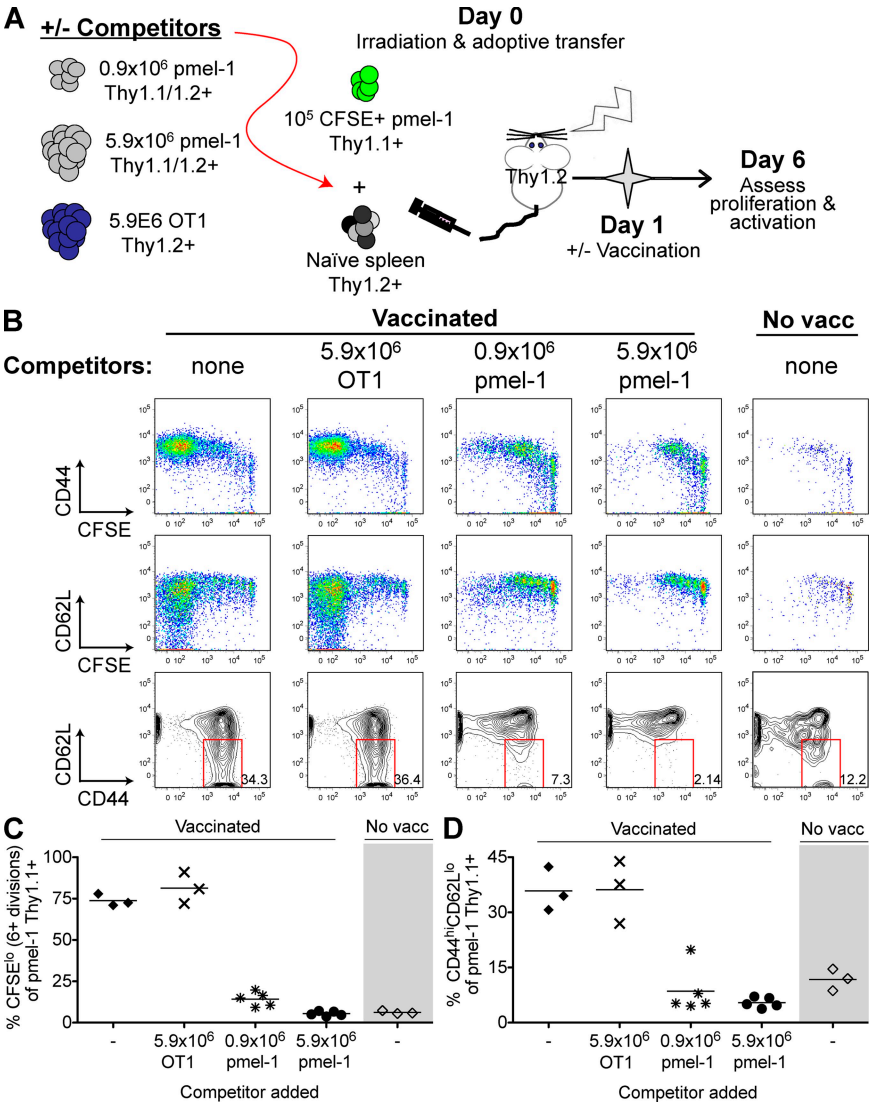

Figure 4. At higher precursor frequency, intraclonal competition limits the initial proliferative burst and acquisition of effector phenotype. (A) Experimental scheme. Mice (n = 3–5/group) underwent sublethal irradiation and adoptive transfer of splenocytes that included 10^5 CFSE-labeled CD8$^+$Thy1.1$^+$ pmel-1 cells. Some groups received competing CD8$^+$Thy1.1$^+$Thy1.2$^+$ pmel-1 cells (0.9×10^6 or 5.9×10^6) or competing CD8$^+$Thy1.2$^+$ OT1 cells (5.9×10^6). 1 d later, mice were vaccinated with hgp100-encoding plasmid, except for a control group that received no vaccination. Vaccine DLNs were harvested from individual mice 5 d after vaccination and proliferation and phenotype of CFSE-labeled CD8$^+$Thy1.1$^+$ pmel-1 cells was assessed. (B) Combined flow cytometric plots of DLNs, gated on CD8$^+$Thy1.1$^+$ pmel-1 cells are shown. Proliferation and phenotypic data for DLNs of individual animals is shown graphically in C and D, respectively. Horizontal line represents mean. P = 0.03 for comparison of vaccinated animals receiving no competitors versus vaccinated animals receiving either high- or low-dose pmel-1 competitors. Representative of two experiments performed under similar conditions.

effector phenotype on the pmel-1 population in mice that had received four different precursor frequencies (Fig. 5). Results consistently demonstrated an inverse correlation between pmel-1 precursor frequency and frequency of $CD44^{hi}CD62L^{lo}LFA\text{-}1^{hi}$ pmel-1 effectors. This is a phenotype that is typical of antigen-experienced cells, and high levels of LFA-1 may not only be important in maintenance of the immunological synapse but may also aid in adhesion of pmel-1 cells at the tumor site (35). Similar trends were seen in the spleen (Fig. 5, B and C) and DLNs (Fig. 5 A). Notably, we have observed a similar inverse correlation between precursor frequency and postvaccination frequency

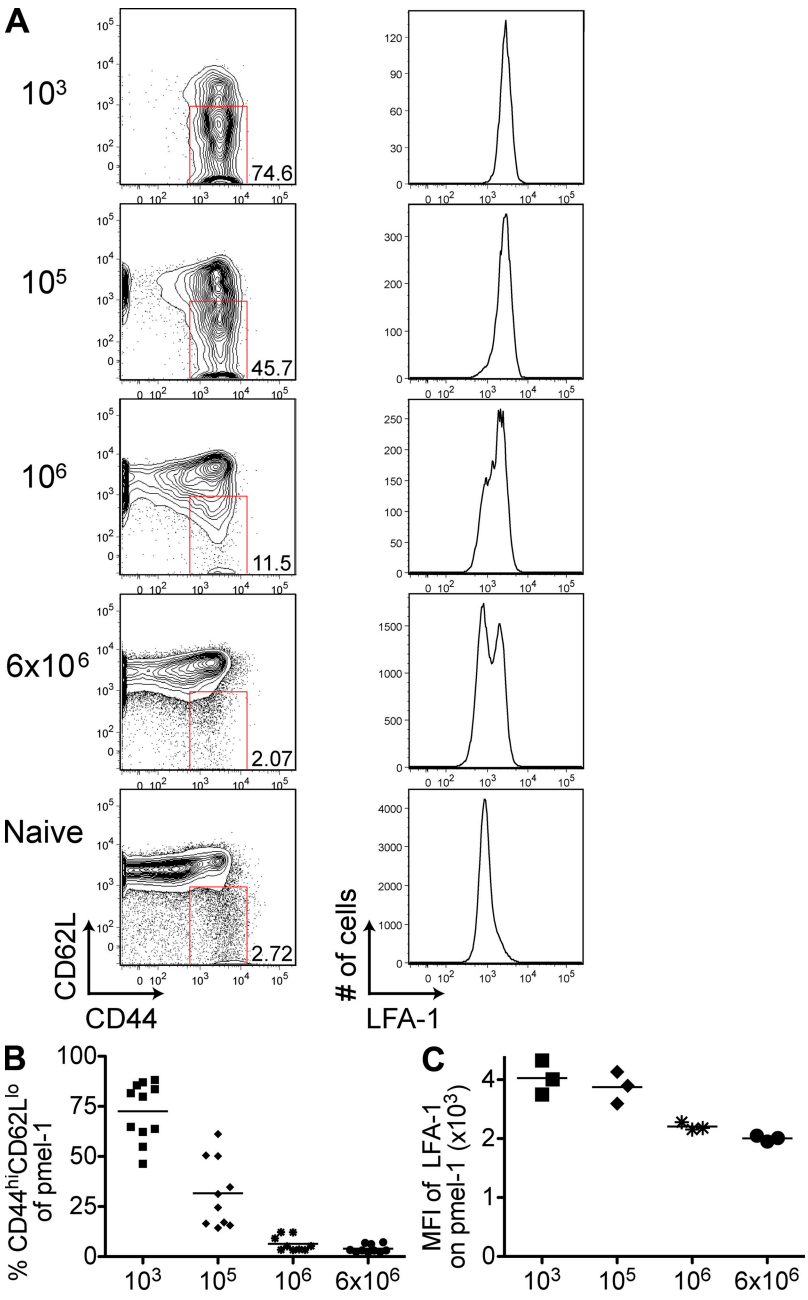

Figure 5. Initial precursor frequency dictates acquisition of vaccine-induced effector phenotype on tumor antigen-specific CD8⁺ T cells. (A) Mice (n = 3/group) were inoculated subcutaneously with B16-matrigel tumors, underwent sublethal irradiation and adoptive transfer 4 d later, and vaccination with hgp100-encoding plasmid the following day. 5 d after vaccination, DLNs and spleens were harvested. Expression of CD44, CD62L, and LFA-1 are shown by flow cytometric contour and histogram plots of pooled DLNs (n = 3 mice/group), and are gated on $CD8^{+}Thy1.1^{+}$ pmel-1 cells. Representative of three experiments. (B) Data shown are from spleens of individual mice in three pooled experiments. $P < 0.001$ for an overall inverse association between the percentage of $CD44^{hi}CD62L^{lo}$ of pmel-1 cells and initial pmel-1 dose. (C) Data shown are from individual spleens of one representative experiment out of three experiments. $P = 0.024$ for an overall inverse association between MFI of LFA-1 on pmel-1 cells and initial pmel-1 dose.

of activated pmel-1 cells after transfer into nonirradiated mice (unpublished data).

These results suggest that the impaired proliferative burst and acquisition of effector phenotype at the high doses are the result of early competition between the pmel-1 transgenic clones. This outcome is consistent with reports of intraclonal competition for foreign antigens (31). This led us to test whether intraclonal competition at the higher pmel-1 input number impaired the gain of antitumor effector function.

Polyfunctional CD8⁺ self-antigen–specific effector cells are generated at low, but not high, initial precursor frequencies

It has been suggested that the high-quality protection elicited by successful CD8⁺ T cell vaccines can be correlated with the generation of populations capable of performing multiple effector functions (36). Thus, the ability of the pmel-1 effector cells located at the tumor, DLNs, and spleen to secrete effector cytokines and to degranulate was investigated. 4 d after B16-matrigel tumor implantation, dose groups were treated and prepared as described in Fig. 3 A, and organs were harvested 5 d after one vaccination with hgp100. Flow cytometry was used to determine IFN-γ and TNF-α production and to assess degranulation by staining for CD107a. We adopted a definition of polyfunctionality as the ability to perform any two of these functions.

Cytokine profiles for gated CD8⁺Thy1.1⁺ pmel-1 cells from tumor and DLN are shown in Fig. 6 A. Effectors generated from 10^3 and 10^5 pmel-1 precursors secreted more IFN-γ and more TNF-α on a population level than those generated

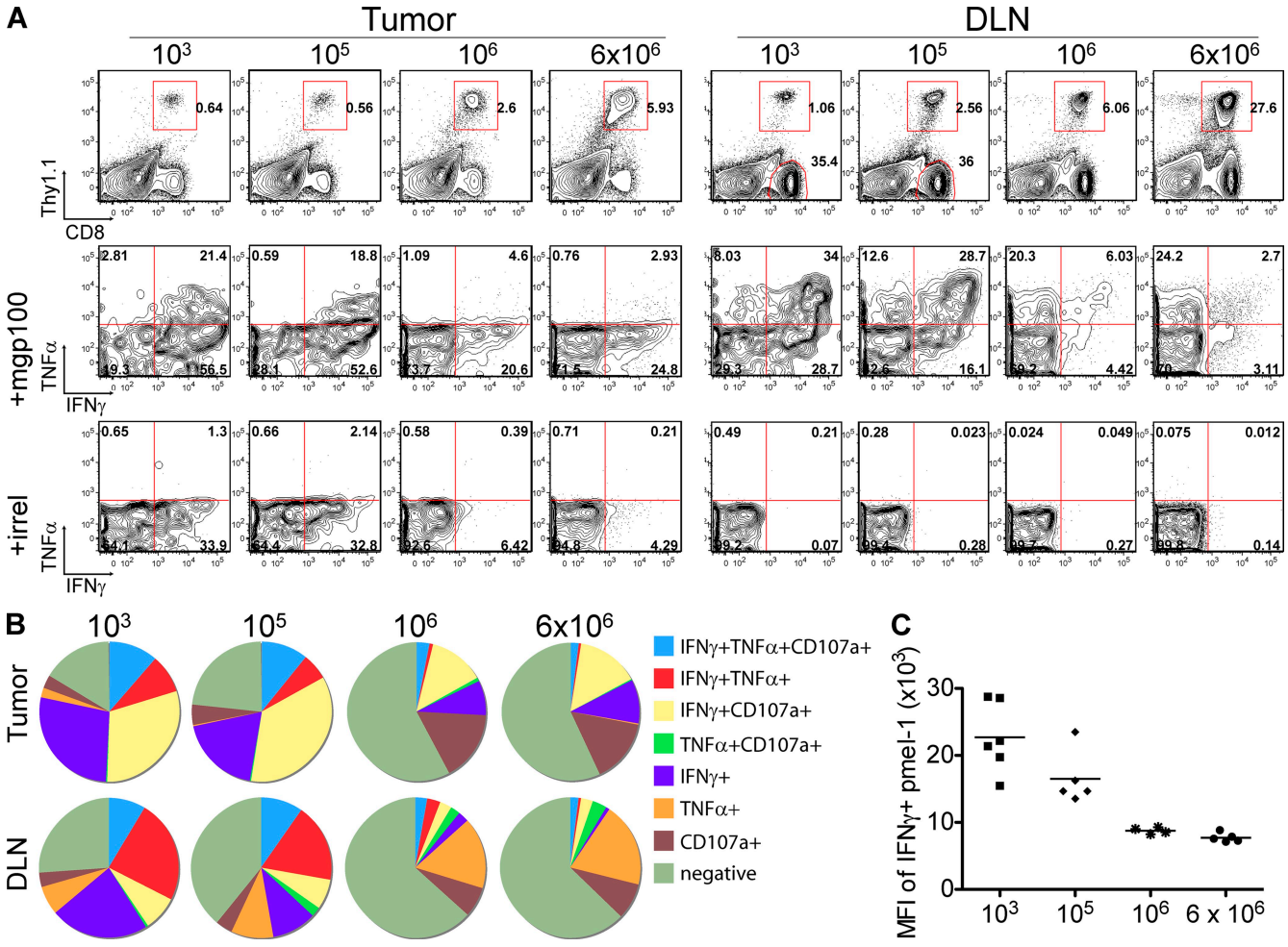

Figure 6. Polyfunctional antigen-specific effector CD8⁺ cells are generated at lower, but not higher, precursor frequencies. (A) Mice (n = 4–6/group) were inoculated subcutaneously with B16-matrigel tumors, and underwent sublethal irradiation and adoptive transfer 4 d later and vaccination with hgp100-encoding plasmid the following day. 5 d after vaccination, tumors, DLNs, and spleens were harvested. Cells were stimulated for 6 h with EL4 cells and either $mgp100_{25-33}$ or irrelevant peptide, and then stained for cytokine production (TNF-α and IFN-γ) and CD107a mobilization. TNF-α and IFN-γ production by gated CD8⁺Thy1.1⁺ pmel-1 cells is shown for pooled tumors and pooled DLNs. (B) Cytokine⁺ and CD107a⁺ cells from A were subject to Boolean gate analysis, and functionality profiles are shown as pie graphs. (C) Graph showing the mean fluorescence intensity (MFI) of IFN-γ for IFN-γ⁺CD8⁺Thy1.1⁺ pmel-1 cells from individual spleens stimulated with $mgp100_{25-33}$. $P < 0.001$ for an overall inverse association between MFI of IFN-γ and initial pmel-1 dose. Shown is one representative experiment out of three experiments (CD107a, IFN-γ) and two experiments (CD107a, IFN-γ, and TNF-α).

from the higher precursor frequencies. The same trend held true, though less strikingly, for CD107a mobilization (Fig. S2, available at http://www.jem.org/cgi/content/full/jem.20081382/DC1). We analyzed the ability of the pmel-1 populations from pooled DLN and tumor to perform one, two, or all three of these functions (Fig. 6 B; mean values ± SD for individual spleens are shown in Fig. S3). In all organs, the effector populations generated from the two lower precursor frequencies were more highly polyfunctional than were populations generated at higher precursor frequencies. Notably, however, the absolute number of polyfunctional effectors was comparable and/or higher at the increased pmel-1 doses (Fig. S4).

These same trends were observed for animals that received vaccination with the self-homologue mouse gp100 (unpublished data). Although the mouse homologue was detectably immunogenic under these conditions, the magnitude of the response, in comparison to that generated with hgp100 vaccination, was lower. We also performed a side-by-side comparison of polyfunctional T cell responses generated from pmel-1 cells transferred into irradiated and naive (nonirradiated) recipients (unpublished data). Similar, although less striking, trends were observed with the exception that in the naive recipient the frequency of $CD107a^+TNF\text{-}\alpha^+IFN\text{-}\gamma^+$ cells was highest in the 10^6 dose group.

Three observations are noteworthy, as they may be directly related to the increased treatment efficacy at lower precursor frequencies. First, after restimulation with irrelevant peptide, a population of $IFN\text{-}\gamma^+$ pmel-1 cells are detected in the tumors of animals receiving lower numbers of pmel-1 cells (Fig. 6 A). Similar levels of $IFN\text{-}\gamma^+$ pmel-1 cells are detected in wells that received no peptide at all (not depicted), suggesting that effector cells generated from lower precursor frequencies are truly functional directly ex vivo. Second, the higher pmel-1 dose groups yielded a greater frequency of effector pmel-1 cells in the DLN that produced only TNF-α (Fig. 6 B). Similarly, a greater frequency of pmel-1 effectors that produced only TNF-α was generated by vaccination with mouse gp100 (unpublished data). The significance of this population is not currently known. Perhaps these cells represent a population that under lower levels of intraclonal competition would also acquire the ability to secrete IFN-γ and/or degranulate. Third, the mean fluorescence intensity of IFN-γ is consistently higher in pmel-1 populations activated at lower precursor frequencies (Fig. 6 C), suggesting the ability to secrete more cytokine. Interestingly, our data suggests that $CD107a^+TNF\text{-}\alpha^+IFN\text{-}\gamma^+$ pmel-1 effectors are cells with higher intensity staining for IFN-γ (Fig. S5, available at http://www.jem.org/cgi/content/full/jem.20081382/DC1). Perhaps the most polyfunctional cells secrete the most cytokine. This observation is consistent with increased MFI of IFN-γ observed for *Leishmania*-specific $CD4^+$ cells in mice (37) and human $CD8^+$ cells against modified vaccinia virus (36).

Therefore, precursor frequency dictates several qualitative aspects of the effector response that are known to be important for tumor eradication.

Distinct "memory" phenotypes are generated from different initial self–antigen–specific precursor frequencies

As antigen is cleared during the resolving effector response, the typical fate of T cell populations is contraction, leaving behind a much smaller population of central and effector memory cells. On the other hand, the process of memory differentiation in the presence of antigen is characterized by stages of exhaustion and/or deletion (38). Recent reports have demonstrated a role for precursor frequency in the generation, subset diversification, and survival of memory cells for foreign antigens (39–41). Therefore, we were interested in determining the phenotypic and functional fate of the pmel-1 memory populations in our treated mice. Indeed, the development of coat depigmentation in our treated mice suggests continued recognition of gp100 self-antigen (Fig. 2, D and E), although it is possible that loss of melanocytes may be a direct consequence of epitope spreading to other melanocyte-specific antigens, and not $gp100_{25\text{-}33}$ recognition-dependent killing.

We phenotyped the pmel-1 populations present at day 85 after vaccination in mice that had survived tumor challenge (Fig. 7 A). Spleens of individual animals were analyzed by flow cytometry, and as was observed during the effector response, the phenotype of the pmel-1 populations looked strikingly different. Pmel-1 $CD44^{hi}CD62L^{lo}$ cells predominated in memory populations generated from low input numbers (Fig. 7 B). One might speculate that the activated effector phenotype acquired by the great majority of pmel-1 cells at the 10^3 dose is maintained because of continued encounter with self-antigen. Therefore, we assessed for functional exhaustion, but did not observe an overt loss of cytokine-secreting abilities in cells harvested and briefly restimulated in vitro at 72 d after vaccination (Fig. 7 C; compare with effector responses shown in Fig. 6 A).

These data indicate that precursor frequency is an important dictator of memory phenotype and function for $CD8^+$ T cells recognizing a self-antigen.

DISCUSSION

Successful immunotherapy of established, poorly immunogenic melanoma tumors has been accomplished in only a few ways (30, 42). In particular, treatment regimens using the adoptive transfer of tumor-specific $CD8^+$ T cells have achieved durable cures (43–45). The quality and quantity of adoptively transferred cells are important parameters when optimizing such a treatment. Many studies to date have focused on aspects of in vitro generation, activation, and expansion of tumor-specific cells for transfer (46–49). Unfortunately, prolonged in vitro culture correlates with impaired in vivo function after transfer (50). Indeed, an in vitro priming and expansion model that completely mimics optimal in vivo effector and memory generation remains elusive. Thus, we chose to explore the transfer of naive, tumor-antigen–specific $CD8^+$ cells that would then be activated in the mouse. We used in vivo administration of an altered-self vaccine to activate our transferred cells at lymph nodes draining the site of disease, as tissue tropism is known to be imparted to T cells during in situ priming (51). Future work comparing the trafficking, persistence,

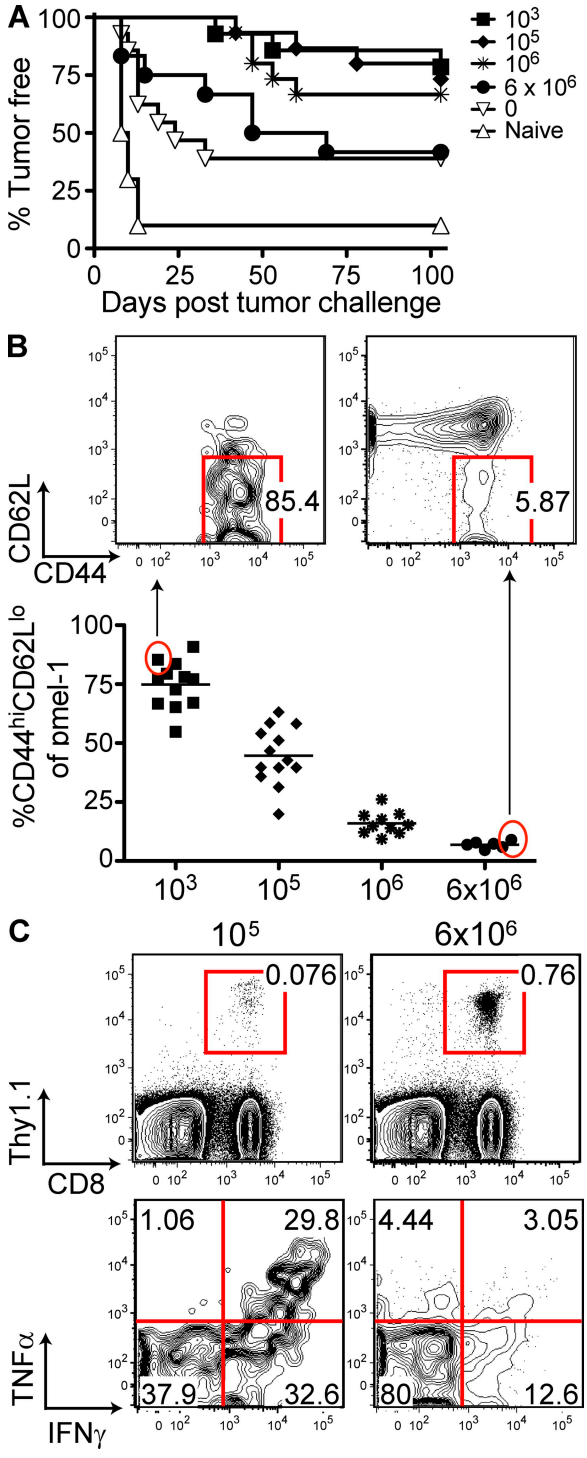

Figure 7. Precursor frequency impacts phenotype of CD8⁺ "memory" populations. Phenotype of pmel-1 CD8⁺ cells was analyzed by flow cytometry ~6 wk after last vaccination. (A) Surviving animals from tumor treatment experiment shown were killed 85 d after the last vaccination. (B) Individual spleens were harvested, stained, and analyzed by flow cytometry for CD44 and CD62L expression on CD8⁺Thy1.1⁺ pmel-1 cells. Dot plots and histograms are shown for representative spleens, and individual values are plotted on graphs. $P < 0.001$ for an inverse overall association between the percentage of $CD44^{hi}CD62L^{lo}$ and initial pmel-1 dose. (C) Naive mice ($n = 2$–3/group) underwent irradiation and adoptive transfer with 10^5 or 6×10^6 pmel-1 cells, received three weekly vaccinations, and were rested for 72 d. DLNs were harvested and cells were stimulated for 6 h with EL4 cells and either $mgp100_{25\text{-}33}$ or irrelevant peptide and stained for cytokine production. TNF-α and IFN-γ staining by gated CD8⁺Thy1.1⁺ pmel-1 cells are shown for representative mice. Data are from at least two independent experiments that were performed under similar conditions.

and efficacy of in vitro–activated versus in vivo–primed tumor-specific cells is warranted.

The initial precursor frequency of foreign antigen–specific T cells in the mouse is low, with reported estimates ranging from 10 to 3,000 cells/mouse (20–26). During the natural immune response to foreign pathogens, these antigen-specific cells expand and, if allowed to subsequently contract as antigen is cleared, will form long-lived memory (52). The resultant effector and memory T cell populations look and behave dramatically different depending on precursor frequency (31, 39–41, 53). Studies addressing the mechanism of this phenomenon illustrate that intraclonal competition for foreign antigens occurs at the level of the APC where clones of the same specificity compete for peptide–MHC complexes (39, 54, 55). Our results demonstrate that the same phenomenon holds true for T cell clones that recognize a tissue-restricted self-antigen. We show that the proliferative burst is stunted at high initial frequencies, as is the acquisition of effector phenotype. We extend published findings to report that precursor frequency dictates acquisition of polyfunctional effector $CD8^+$ T cells. Priming at low precursor frequency generated a greater frequency of $IFN\text{-}\gamma^+TNF\text{-}\alpha^+CD107a^+$ cells, which were present at both the tumor site and draining lymph node.

Most significantly, eradication of B16 melanoma tumors is impaired at high initial frequencies. Our data suggest that this is the negative consequence of priming T cells at supraphysiological precursor frequencies and we believe this is clinically relevant information. We predict the same negative consequences in models where mice are challenged with foreign pathogens. Thus, clinical protocols designed to activate adoptively transferred $CD8^+$ T cells should consider these effects.

Several published reports address the frequency of the human T cells specific for the melanoma differentiation antigen Melan-A/MART-1 restricted to HLA-A*0201, and the melanoma cancer testes antigen $MAGE\text{-}3_{168\text{-}176}$ presented on HLA-A1. Using tetramer staining, Pittet et al. described a surprisingly high frequency (~1 in 2,500 $CD8^+$ T cells) of Melan-A/MARTI-1–specific T cells in some, but not all, healthy, HLA-A*0201⁺ individuals (56). Later, it was shown that the majority of this population was not functionally reactive to Melan-A/MART-1, but rather to similar peptide analogues (57). It is unclear how commonly this phenomenon occurs in the T cell repertoire against self. The frequency of anti–MAGE-3–specific $CD8^+$ T cells in an individual without cancer was estimated to be much lower, 6×10^{-7}, with a repertoire consisting of an estimated >100 different

clonotypes (58). Anti–MAGE-3 vaccine induced detectable $CD8^+$ T cell responses in some patients, and most of these responses were monoclonal (59, 60). Interestingly, we also observed a very restricted vaccine-induced anti-$gp100_{25\text{-}33}$ response in mice that was limited to between 1 and 4 responding TCR Vβ per mouse.

Our estimate of endogenous $gp100_{25\text{-}33}$ clonal frequency is, to our knowledge, the lowest reported for any mouse antigen. To estimate precursor frequency, we adopted a method of indirect determination initially reported by Blattman et al. (23). We recognize that this method assumes that preimmune transgenic cells and endogenous antigen-specific precursors have similar propensities to enter the response, undergo similar priming, and possess similar expansion and differentiation capabilities. Unfortunately, we cannot rule out the possibility that endogenous clones may respond to antigen in a qualitatively and quantitatively different manner than pmel-1 cells. We tested and compared recognition of $mgp100_{25\text{-}33}$ by pmel-1 cells and endogenous responders, by analyzing frequency of IFN-γ cells relative to titrating peptide. Using this surrogate measure of affinity, we found that the pmel-1 clone is of higher avidity than at least six (of seven tested) endogenous clones (unpublished data). Thus, we must consider that low precursor frequency and/or low TCR avidity may explain the impairment in B16 melanoma eradication in animals that do not receive pmel-1 cells.

It was recently demonstrated that even a single cell can give rise to multiple effector and memory lineages, perhaps by asymmetrical cell division (61, 62). However, our results suggest that a sizeable proliferative burst is needed to destroy a progressively growing malignancy. Indeed, populations of greater initial size might simply have a kinetic advantage. This concept is modeled in Fig. 8. We propose that the optimal precursor frequency for generating high-quality antitumor $CD8^+$ responses can be reached by using adoptive transfer to supplement the naive repertoire. However, when clonal frequency rises above a certain threshold, competition diminishes the quality of the antitumor immune response.

This model (Fig. 8) raises many questions. How similar is this dose-response curve for $CD8^+$ T cells recognizing foreign antigens? For $CD8^+$ T cells recognizing other self-antigens? For $CD8^+$ T cells primed in the nonirradiated host? Although preliminary data suggest that intraclonal pmel-1 cell competition is operative in the nonirradiated animal,

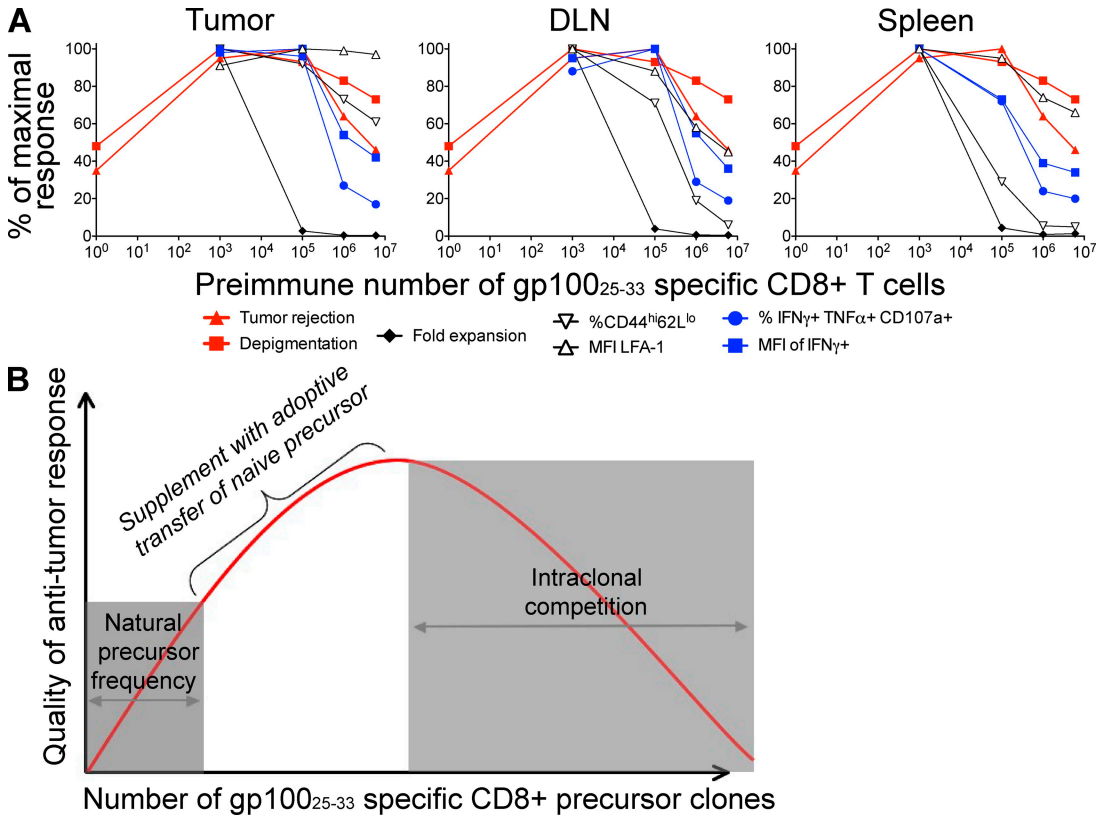

Figure 8. A model for the impact of antigen-specific precursor frequency on the quality of antitumor responses. (A) The mean values for parameters shown were calculated for experimentally tested pmel-1 dose groups (0, 10^3, 10^5, 10^6, and 6×10^6). For each parameter, the maximal response was set at 100%, and responses for other pmel-1 dose groups were calculated as a percentage of this maximum. Values from spleen, DLN, and tumor are shown graphically. (B) Model based on A. The x axis shows the number of naive tumor antigen–specific $CD8^+$ T cells present at the time of vaccine administration. The y axis is the quality of the antitumor immune response. The curve demonstrates that there is an optimal precursor frequency for generating the strongest antitumor response.

there appears to be an approximate 1-log difference in the effect when compared with irradiated animals (unpublished data). Further study will be aimed at exploring the detailed differences observed in the naive versus irradiated recipient.

Notably, in one study, at high precursor frequencies, more $CD4^+$ T cells were shown to enter the response simply by providing more antigen (63). Conversely, limiting the effective antigen dose by addition of monoclonal antibody specific for a particular MHC–peptide complex impaired the differentiation of peptide-specific memory cells (39). Thus, there seems to be built-in regulation of the size of the immune response depending on the "size" of the antigenic insult. It is predicted that increasing antigen dose would raise the threshold where pmel-1 intraclonal competition becomes operative, whereas decreasing antigen would lower it. However, the possibility that increasing antigen dose may limit the efficacy of vaccine-generated antitumor immunity must also be considered. Greater antigen availability may allow for recruitment of increased numbers of endogenous, and for lower affinity clones, leading to a comparative decrease in tumor killing.

It is likely that at all stages of an immune response, reactive lymphocytes require many resources that are naturally limiting. These resources include antigen, but might also include costimulation, cytokines, other survival signals, and CD4 help (64). We hypothesize that the absence/presence and levels of these other variables modulate the curve presented in Fig. 8. Current and future work will address the relevance of these, most of which are easily delivered by plasmid and gene gun (9, 65). Lastly, it is well documented that under certain conditions, the TCR repertoire is less diverse (19). During aging, HIV infection, or in the posttransplant setting, reactivity to $gp100_{25\text{-}33}$ might be lost because of deficiencies in the repertoire.

It is intriguing that precursor frequency dictates polyfunctionality of the pmel-1 effector T cell response generated by vaccination in our model. Recent advances in multiparameter flow cytometry have enabled the study of both the phenotype and function of human $CD8^+$ T cells in the setting of chronic viral infection; with and without the addition of experimental vaccines. However, the correlates of protection for $CD8^+$ T cell mediated vaccination against either chronic infection, such as HIV or tumors, are not yet clearly defined (66). Current experts argue that it is not enough to simply monitor the magnitude of vaccine-induced $CD8^+$ T cell response, such as the frequency of IFN-γ^+ cells by ELISPOT (67). To understand the best $CD8^+$ T cell correlates of tumor protection, we must understand the T cell response in its entirety—that is the patterns of production of multiple cytokines and chemokines. We believe that further exploration into the effector response generated in our model may be useful in defining $CD8^+$ T cell correlates of antitumor protection. Whether polyfunctional cells actually cause disease regression or are simply a consequence thereof will require the study of mouse and nonhuman primate models, where outcomes and responses can be easily manipulated. For example, are polyfunctional $CD8^+$ T cells better just because of their increased functions or because they are superior at an individual function? Future studies should address whether these cells actually do produce more of each individual cytokine and whether this cytokine is responsible for antitumor and viral outcomes.

It is both puzzling and intriguing that the absolute number of activated ($CD44^{hi}CD62L^{lo}$) effectors with the ability to secrete cytokines or degranulate is not greater at the lower precursor frequencies, despite the improved efficacy of these frequencies (Fig. S4 and not depicted). The decreased tumor growth observed in these animals may be correlated with an as yet undefined effector capability. For example, these effectors may be better at penetrating the tumor mass, or they may be less susceptible to suppression by regulatory T or myeloid cells at the tumor site. Another attractive hypothesis is that effectors generated from the lower doses are of higher functional avidity, such that they are better capable of recognizing B16 melanoma tumors that presumably express low levels of MHC–$gp100_{25\text{-}33}$ peptide complexes. Others have hypothesized that only a small number of effectors might be capable of initiating tumor rejection, which is performed by the active recruitment of other immune effector cells (60). Perhaps we might detect significant numbers of $CD8^+$ and/or $CD4^+$ T cells specific for other melanoma antigens in animals that receive lower precursor frequency pmel-1 cells and subsequently reject tumor. This is currently under investigation.

Alternatively, the presence of large numbers of unactivated pmel-1 cells at the higher doses may directly or indirectly inhibit the response of those few activated effectors. Recent reports have identified and characterized a population of IL-10–secreting, $CD8^+$ suppressor cells in naive mice (68, 69). These cells are distinguished by high levels of CD122 (IL-2/-15Rβ). Notably, we detected high levels of CD122 on pmel-1 "memory" populations generated from high precursor frequencies in vaccinated animals (not depicted). In contrast, CD122 expression on memory pmel-1 populations generated from lower precursor frequencies (10^3 or 10^5 pmel-1 cells) ranged from uniformly low to negative. Notably, the memory population in animals receiving 10^5 pmel-1 cells, but no vaccination, also displayed high levels of CD122. Perhaps weak self-reactivity, as is expected for homeostatically expanded but nonvaccinated pmel-1 cells, leads to CD122 up-regulation. Whether these cells have functional properties similar to published $CD8^+CD122^+$ suppressors remains to be established, and ongoing experiments are aimed at testing this hypothesis as well.

Promising clinical trials have tested infusion of autologous T cells into lymphoablated patients, in some cases combined with vaccination (70–74). Sources of tumor-reactive T cells have included autologous tumor infiltrating lymphocytes, autologous PBL cells, and vaccine-primed autologous T cells from blood or DLNs (43, 45). Current strategies using adoptive immunotherapy in the clinical setting of cancer are based on the premise that "more" is better with great effort spent in the generation of tens of billions of antitumor T cells for transfer. To our knowledge, all reports involved ex vivo manipulation to activate and/or expand the tumor-reactive T

cells. Our results show that combining lymphodepletion with physiologically relevant numbers of naive tumor-specific $CD8^+$ cells and in vivo administration of an effective vaccine generates a high-quality, antitumor response in mice. This approach requires strikingly low numbers of naive tumor-specific cells, making it a new and truly potent treatment strategy. Emerging technologies, notably lentiviral gene transfer, make it possible to genetically arm T cells with tumor specificity without the need for overt activation (75). We recommend that future trials combining adoptive immunotherapy and vaccination explore an in vivo activation strategy such as the one we present here. Care should be taken when formulating the dose of transferred cells, which, when modulated, may turn an ineffective treatment into one which results in robust tumor control.

MATERIALS AND METHODS

Mice and tumors. Mouse work was performed in accordance with institutional guidelines under a protocol approved by Memorial Sloan-Kettering Cancer Center Institutional Animal Care and Use Committee. All mice were maintained in a pathogen-free facility according to National Institutes of Health Animal Care guidelines. C57BL/6J mice (females, 6–10 wk old) were purchased from The Jackson Laboratory. Pmel-1 TCR transgenic mice have been reported (30) and were bred with $Thy1.1^+$ C57BL/6J mice (76) (The Jackson Laboratory) as a source of tumor-specific $CD8^+$ T cells. For some experiments, $Thy1.1^+/Thy1.2^+$ Pmel-1 TCR transgenic mice were generated and used as a source of otherwise identical tumor-specific $CD8^+$ T cells.

The mouse melanoma cell line B16F10 (hereafter referred to as "B16") was originally obtained from I. Fidler (M.D. Anderson Cancer Center, Houston, TX). Cells were cultured as previously described (77). For experiments where rejection and growth of tumors were monitored, 10^5 (or 1.25×10^5 for some experiments) live cells were intradermally injected in the shaved flank of mice. Tumor growth was monitored by inspection with calipers 3–4 times/wk, and mice were killed when tumors ulcerated and/or reached 1 cm in diameter.

B16 cells mixed with Matrigel Basement Membrane Matrix, Growth Factor Reduced (BD) were subcutaneously inoculated in the shaved flank of mice for experiments where tumors were later harvested for analysis of tumor-infiltrating immune cells.

To assess coat depigmentation in mice that rejected tumor, animals were anaesthetized and abdomens were scanned with a Hewlett-Packard Series 650 scanner and HP PrecisionScanPro software. Resolution for all images was lowered to accommodate images of individual mice <100 MB in size. Average pixels were quantified with UN-SCAN-IT gel software, version 4.3 (Silk Scientific, Inc.). In brief, four similarly sized quadrants were subjected to segment analysis for each animal and the mean number of pixels per segment area was calculated.

Irradiation and adoptive transfer. Recipient mice received 600 cGy total body irradiation from a ^{137}Cs source several hours before adoptive transfer. Transgenic pmel-1 donor mice were 6–12-wk-old females that had yet to begin showing signs of coat depigmentation. $CD8^+$ T cells were purified from spleen and subcutaneous lymph nodes using EasySep Mouse $CD8^+$ T Cell Enrichment kits, according to the manufacturer's suggested protocol with two rounds of negative selection through an EasySep Magnet (StemCell Technologies). $CD8^+$ purity was assessed by flow cytometry and was typically between 87–95%. For adoptive transfer, dose groups were washed twice with PBS, resuspended at 30 million cells per 200 μl, and injected via lateral vein into irradiated recipient animals. Dose groups were confirmed by flow cytometry, as was the naive phenotype of pmel-1 donors with $CD44^{lo}CD62L^{hi}$ percentages similar to naive, wild-type $CD8^+$ T cells.

Plasmid constructs and DNA immunization. The WRG/BEN vector construct containing hgp100 was used for immunizing against mgp100 (10, 12). The same vector backbone containing mgp100 was used in some experiments. An ovalbumin–minigene construct, described previously (12), was used for priming SIINFEKL-specific responses. Vaccine was prepared by coating 1.5-μM gold particles (Alfa Aesar) with purified DNA, and precipitated onto bullets of Teflon tubing (1 μg plasmid/bullet). A high-pressure, helium-driven gene gun (Accell; PowderMed) was used for cutaneous particle bombardment of DNA into mouse skin. In brief, mouse hair was removed by depilation, and one bullet was delivered to each abdominal quadrant for a total of 4 μg plasmid/mouse (9).

TCR Vβ determination. One-third of total spleen and lymph nodes cells from individual mice with positive responses to vaccine were stained with hgp100-tetramer and FITC-conjugated antibodies specific for TCR-β families (Mouse Vβ TCR Screening Panel; BD). Remaining cells from these same mice were enriched for $CD8^+$ with EasySep Mouse $CD8^+$ T Cell Enrichment kits and one round of negative selection through an EasySep Magnet (Stem Cell Technologies). Samples were FACS sorted to yield ~99% pure hgp100-tetramer$^+CD8^+$ populations and total RNA was extracted with an RNeasy Micro kit (QIAGEN). Each sample was reverse transcribed with a High Capacity cDNA Archive kit (Applied Biosystems). PCR amplification of CDR3 regions was performed with family-specific Vβ forward primers and a TCR-β constant region-specific reverse primer designed by P. Savage (78). Reactions were performed with annealing at 55°C, for 20–40 cycles. PCR products were cloned into pCR4-TOPO vector with TOPO TA Cloning kit for sequencing (Invitrogen) and sequenced by standard methods. TCR Jβ and CDR3 regions were classified and reported using the International ImMunoGeneTics Information System nomenclature (79).

Isolation of lymphocytes from tumors. Subcutaneous B16-Matrigel tumors were inoculated as described in Materials and methods and removed by dissection at various time points after treatment. Tumor tissue was digested with 2 mg/ml Collagenase D (Roche) and 1 mg/ml DNase I (Sigma-Aldrich) for 1 h at 37 degrees, passed through 40-μM filters, and mononuclear cells were isolated by density gradient centrifugation. In brief, cell pellets were resuspended in 80% Percoll (GE Healthcare), overlaid with 40%, and the interface was isolated after 30 min of room temperature centrifugation. Cells were washed twice, and if necessary, RBC lysis was performed with ammonium chloride lysis buffer (1.5 M NH_4Cl, 10 mM EDTA disodium salt, and 100 mM $NaHCO_3$).

Flow cytometry. The following fluorochrome-conjugated antibodies were purchased from BD: anti-Vβ13 (MR12-3), Vβ5.1/5.2 (MR9-4), CD3e (145-2C11), CD62L (MEL-14), CD4 (RM4-5), CD8a (53–6.7), Thy1.1 (HIS51 and OX-7), Thy1.2 (53–2.1), CD107a (1D4B), TNF-α (MP6-XT22), IFN-γ (XMG1.2), CD122 (TM-β1), CD19 (1D3), and Ki67 (B56).

Other antibodies were purchased from eBioscience: CD44 (IM7), CD62L (MEL-14), and LFA-1α (M17/4). Anti-mouse CD8a (5H10) was purchased from Invitrogen.

Surface staining using antibody quantities predetermined by titration experiments was performed in a total volume of 100 μl PBS containing 1% BSA on ice for 20–30 min in the dark. Cells were washed twice before and after staining. All surface stains were performed following blockade of FCγIII/II receptor with purified, unlabeled antibody (clone 2.4G2; BD). Before acquisition, cells were resuspended in DAPI (Invitrogen) to permit dead cell exclusion. Samples were acquired and electronically compensated on a LSR II (BD), and exported for analysis in FlowJo (Tree Star, Inc.).

In some cases, gp100-reactive $CD8^+$ cells were identified by staining with PE-conjugated tetramer containing the D^b epitope from hgp100, KVPRNQDWL (12) purchased from Beckman Coulter. $Hgp100_{25-33}$ peptide was used for production rather than self-mouse peptide because only the higher affinity peptides were able to form tetramers. Cells were washed and stained at room temperature in PBS containing 1% BSA and anti-CD8 clone 53–6.7 was always chosen for use when staining for tetramer. In some experiments, a channel for

$CD4^+$ and $CD19^+$ cells was used to exclude background staining and enhance detection of low-frequency $Tetramer^+CD8^+$ cells.

Intracellular cytokine and CD107a mobilization assay. Cells were stimulated with 1 μg/ml peptide in the presence of EL-4 cells, at a ratio of 10 or 20:1, in complete RPMI 1640 medium containing 7.5% FBS. For simultaneous detection of CD107a and TNF-α, both Brefeldin A (BFA) and monesin secretion inhibitors were added to the culture after one hour incubation (80). After 6 h of incubation, samples were stained for surface markers. Cells were then fixed and permeabilized using Cytofix/Cytoperm kit (BD) according to the manufacturer's instructions, stained for intracellular TNF-α and IFN-γ, and analyzed on a LSR II flow cytometer (BD).

To determine whether antigen-specific $CD8^+$ pmel-1 cells were capable of one, two, or three functions (CD107a mobilization, and/or secretion of either TNF-α and IFN-γ). Boolean Gate analysis was performed in FlowJo (Tree Star, Inc.).

Statistical calculations. Six treatment strategies were assessed comprising five treatment group (pmel-1 doses) and one control group (naive). Because of the small sample sizes, comparisons between treatment strategies were assessed using the Mann-Whitney U (two groups) or Kruskal-Wallis (more than two groups) tests. Because of the exploratory nature of these analyses, results were not adjusted for multiple comparisons, unless otherwise indicated. Tumor-free survival curves were estimated using the Kaplan-Meier method and comparisons between groups were made using the Mann-Whitney U test because all mice were followed to the study end date.

Online supplemental material. Fig. S1 shows flow cytometric contour plots for individual vaccinated animals (receiving either 0 or 10 pmel-1 cells) that were used to estimate endogenous $gp100_{25\text{-}33}$–reactive $CD8^+$ T cell precursor frequency. In Fig. S2, tumor and DLN pmel-1 cell CD107a mobilization for different starting precursor frequencies is shown. Fig. S3 depicts polyfunctionality profiles for splenic pmel-1 cells, while Fig. S4 shows the absolute number of these same sub-groups. Overlaid staining intensity for IFN-γ produced by mono- and polyfunctional pmel-1 sub-groups is shown in Fig. S5. Online supplemental material is available at http://www.jem.org/cgi/content/full/jem.20081382/DC1.

The authors wish to thank Stephanie Terzulli, David Posnett, Mary Jo Turk, Francesca Avogadri, Pete Savage, Sergio Quezada, Emily Corse, and especially John Markley for comments, careful reading, and editing of this manuscript.

This work was supported by National Institutes of Health grants R01CA56821, P01CA33049, and P01CA59350 (to A.N. Houghton), MSTP grant GM07739 (G.A. Rizzuto), NIH CA10260 (to M.-A. Perales); Swim Across America; the Mr. William H. Goodwin and Mrs. Alice Goodwin and the Commonwealth Cancer Foundation for Research and the Experimental Therapeutics Center of Memorial Sloan-Kettering Cancer Center (to A.N. Houghton and J.D. Wolchok). G.A. Rizzuto received support from the Cancer Research Institute (New York) Pre-Doctoral Fellowship. A.M. Lesokhin is supported by Clinical Scholars Biomedical Research Training Program T32 CA009512.

The authors have no conflicting interests.

Submitted: 26 June 2008
Accepted: 6 March 2009

REFERENCES

1. Sant'Angelo, D.B., P.G. Waterbury, B.E. Cohen, W.D. Martin, L. Van Kaer, A.C. Hayday, and C.A. Janeway Jr. 1997. The imprint of intrathymic self-peptides on the mature T cell receptor repertoire. *Immunity*. 7:517–524.
2. Barton, G.M., C. Beers, P. deRoos, S.R. Eastman, M.E. Gomez, K.A. Forbush, and A.Y. Rudensky. 2002. Positive selection of self-MHC-reactive T cells by individual peptide-MHC class II complexes. *Proc. Natl. Acad. Sci. USA*. 99:6937–6942.
3. Zehn, D., and M.J. Bevan. 2006. T cells with low avidity for a tissue-restricted antigen routinely evade central and peripheral tolerance and cause autoimmunity. *Immunity*. 25:261–270.
4. Houghton, A.N. 1994. Cancer antigens: immune recognition of self and altered self. *J. Exp. Med*. 180:1–4.
5. Boon, T., P.G. Coulie, B.J. Van den Eynde, and P. van der Bruggen. 2006. Human T cell responses against melanoma. *Annu. Rev. Immunol*. 24:175–208.
6. Theos, A.C., S.T. Truschel, G. Raposo, and M.S. Marks. 2005. The Silver locus product Pmel17/gp100/Silv/ME20: controversial in name and in function. *Pigment Cell Res*. 18:322–336.
7. Naftzger, C., Y. Takechi, H. Kohda, I. Hara, S. Vijayasaradhi, and A.N. Houghton. 1996. Immune response to a differentiation antigen induced by altered antigen: a study of tumor rejection and autoimmunity. *Proc. Natl. Acad. Sci. USA*. 93:14809–14814.
8. Guevara-Patino, J.A., M.E. Engelhorn, M.J. Turk, C. Liu, F. Duan, G. Rizzuto, A.D. Cohen, T. Merghoub, J.D. Wolchok, and A.N. Houghton. 2006. Optimization of a self antigen for presentation of multiple epitopes in cancer immunity. *J. Clin. Invest*. 116:1382–1390.
9. Engelhorn, M.E., J.A. Guevara-Patino, G. Noffz, A.T. Hooper, O. Lou, J.S. Gold, B.J. Kappel, and A.N. Houghton. 2006. Autoimmunity and tumor immunity induced by immune responses to mutations in self. *Nat. Med*. 12:198–206.
10. Weber, L.W., W.B. Bowne, J.D. Wolchok, R. Srinivasan, J. Qin, Y. Moroi, R. Clynes, P. Song, J.J. Lewis, and A.N. Houghton. 1998. Tumor immunity and autoimmunity induced by immunization with homologous DNA. *J. Clin. Invest*. 102:1258–1264.
11. Wolchok, J.D., J. Yuan, A.N. Houghton, H.F. Gallardo, T.S. Rasalan, J. Wang, Y. Zhang, R. Ranganathan, P.B. Chapman, S.E. Krown, et al. 2007. Safety and immunogenicity of tyrosinase DNA vaccines in patients with melanoma. *Mol. Ther*. 15:2044–2050.
12. Gold, J.S., C.R. Ferrone, J.A. Guevara-Patino, W.G. Hawkins, R. Dyall, M.E. Engelhorn, J.D. Wolchok, J.J. Lewis, and A.N. Houghton. 2003. A single heteroclitic epitope determines cancer immunity after xenogeneic DNA immunization against a tumor differentiation antigen. *J. Immunol*. 170:5188–5194.
13. Rosenberg, S.A., J.C. Yang, and N.P. Restifo. 2004. Cancer immunotherapy: moving beyond current vaccines. *Nat. Med*. 10:909–915.
14. Dummer, W., A.G. Niethammer, R. Baccala, B.R. Lawson, N. Wagner, R.A. Reisfeld, and A.N. Theofilopoulos. 2002. T cell homeostatic proliferation elicits effective antitumor autoimmunity. *J. Clin. Invest*. 110:185–192.
15. Jorritsma, A., A.D. Bins, T.N. Schumacher, and J.B. Haanen. 2008. Skewing the T-cell repertoire by combined DNA vaccination, host conditioning, and adoptive transfer. *Cancer Res*. 68:2455–2462.
16. Gattinoni, L., S.E. Finkelstein, C.A. Klebanoff, P.A. Antony, D.C. Palmer, P.J. Spiess, L.N. Hwang, Z. Yu, C. Wrzesinski, D.M. Heimann, et al. 2005. Removal of homeostatic cytokine sinks by lymphodepletion enhances the efficacy of adoptively transferred tumor-specific CD8+ T cells. *J. Exp. Med*. 202:907–912.
17. Paulos, C.M., C. Wrzesinski, A. Kaiser, C.S. Hinrichs, M. Chieppa, L. Cassard, D.C. Palmer, A. Boni, P. Muranski, Z. Yu, et al. 2007. Microbial translocation augments the function of adoptively transferred self/tumor-specific CD8+ T cells via TLR4 signaling. *J. Clin. Invest*. 117:2197–2204.
18. Klebanoff, C.A., H.T. Khong, P.A. Antony, D.C. Palmer, and N.P. Restifo. 2005. Sinks, suppressors and antigen presenters: how lymphodepletion enhances T cell-mediated tumor immunotherapy. *Trends Immunol*. 26:111–117.
19. Nikolich-Zugich, J., M.K. Slifka, and I. Messaoudi. 2004. The many important facets of T-cell repertoire diversity. *Nat. Rev. Immunol*. 4:123–132.
20. Casrouge, A., E. Beaudoing, S. Dalle, C. Pannetier, J. Kanellopoulos, and P. Kourilsky. 2000. Size estimate of the alpha beta TCR repertoire of naive mouse splenocytes. *J. Immunol*. 164:5782–5787.
21. Moon, J.J., H.H. Chu, M. Pepper, S.J. McSorley, S.C. Jameson, R.M. Kedl, and M.K. Jenkins. 2007. Naive CD4(+) T cell frequency varies for different epitopes and predicts repertoire diversity and response magnitude. *Immunity*. 27:203–213.
22. Obar, J.J., K.M. Khanna, and L. Lefrancois. 2008. Endogenous naive CD8+ T cell precursor frequency regulates primary and memory responses to infection. *Immunity*. 28:859–869.
23. Blattman, J.N., R. Antia, D.J. Sourdive, X. Wang, S.M. Kaech, K. Murali-Krishna, J.D. Altman, and R. Ahmed. 2002. Estimating the pre-

cursor frequency of naive antigen-specific CD8 T cells. *J. Exp. Med.* 195:657–664.
24. Butz, E.A., and M.J. Bevan. 1998. Massive expansion of antigen-specific CD8+ T cells during an acute virus infection. *Immunity.* 8:167–175.
25. Bousso, P., A. Casrouge, J.D. Altman, M. Haury, J. Kanellopoulos, J.P. Abastado, and P. Kourilsky. 1998. Individual variations in the murine T cell response to a specific peptide reflect variability in naive repertoires. *Immunity.* 9:169–178.
26. Whitmire, J.K., N. Benning, and J.L. Whitton. 2006. Precursor frequency, nonlinear proliferation, and functional maturation of virus-specific CD4+ T cells. *J. Immunol.* 176:3028–3036.
27. Cao, W., B.A. Myers-Powell, and T.J. Braciale. 1996. The weak CD8+ CTL response to an influenza hemagglutinin epitope reflects limited T cell availability. *J. Immunol.* 157:505–511.
28. Daly, K., P. Nguyen, D.L. Woodland, and M.A. Blackman. 1995. Immunodominance of major histocompatibility complex class I-restricted influenza virus epitopes can be influenced by the T-cell receptor repertoire. *J. Virol.* 69:7416–7422.
29. Goodnow, C.C., J. Sprent, B. Fazekas de St Groth, and C.G. Vinuesa. 2005. Cellular and genetic mechanisms of self tolerance and autoimmunity. *Nature.* 435:590–597.
30. Overwijk, W.W., M.R. Theoret, S.E. Finkelstein, D.R. Surman, L.A. de Jong, F.A. Vyth-Dreese, T.A. Dellemijn, P.A. Antony, P.J. Spiess, D.C. Palmer, et al. 2003. Tumor regression and autoimmunity after reversal of a functionally tolerant state of self-reactive CD8+ T cells. *J. Exp. Med.* 198:569–580.
31. Badovinac, V.P., J.S. Haring, and J.T. Harty. 2007. Initial T cell receptor transgenic cell precursor frequency dictates critical aspects of the CD8(+) T cell response to infection. *Immunity.* 26:827–841.
32. Dudley, M.E., and S.A. Rosenberg. 2003. Adoptive-cell-transfer therapy for the treatment of patients with cancer. *Nat. Rev. Cancer.* 3:666–675.
33. Overwijk, W.W., A. Tsung, K.R. Irvine, M.R. Parkhurst, T.J. Goletz, K. Tsung, M.W. Carroll, C. Liu, B. Moss, S.A. Rosenberg, and N.P. Restifo. 1998. gp100/pmel 17 is a murine tumor rejection antigen: induction of "self"-reactive, tumoricidal T cells using high-affinity, altered peptide ligand. *J. Exp. Med.* 188:277–286.
34. Goldrath, A.W., L.Y. Bogatzki, and M.J. Bevan. 2000. Naive T cells transiently acquire a memory-like phenotype during homeostasis-driven proliferation. *J. Exp. Med.* 192:557–564.
35. Smith, A., P. Stanley, K. Jones, L. Svensson, A. McDowall, and N. Hogg. 2007. The role of the integrin LFA-1 in T-lymphocyte migration. *Immunol. Rev.* 218:135–146.
36. Precopio, M.L., M.R. Betts, J. Parrino, D.A. Price, E. Gostick, D.R. Ambrozak, T.E. Asher, D.C. Douek, A. Harari, G. Pantaleo, et al. 2007. Immunization with vaccinia virus induces polyfunctional and phenotypically distinctive CD8(+) T cell responses. *J. Exp. Med.* 204:1405–1416.
37. Darrah, P.A., D.T. Patel, P.M. De Luca, R.W. Lindsay, D.F. Davey, B.J. Flynn, S.T. Hoff, P. Andersen, S.G. Reed, S.L. Morris, et al. 2007. Multifunctional TH1 cells define a correlate of vaccine-mediated protection against Leishmania major. *Nat. Med.* 13:843–850.
38. Wherry, E.J., D.L. Barber, S.M. Kaech, J.N. Blattman, and R. Ahmed. 2004. Antigen-independent memory CD8 T cells do not develop during chronic viral infection. *Proc. Natl. Acad. Sci. USA.* 101:16004–16009.
39. Blair, D.A., and L. Lefrancois. 2007. Increased competition for antigen during priming negatively impacts the generation of memory CD4 T cells. *Proc. Natl. Acad. Sci. USA.* 104:15045–15050.
40. Marzo, A.L., K.D. Klonowski, A. Le Bon, P. Borrow, D.F. Tough, and L. Lefrancois. 2005. Initial T cell frequency dictates memory CD8+ T cell lineage commitment. *Nat. Immunol.* 6:793–799.
41. Hataye, J., J.J. Moon, A. Khoruts, C. Reilly, and M.K. Jenkins. 2006. Naive and memory CD4+ T cell survival controlled by clonal abundance. *Science.* 312:114–116.
42. van Elsas, A., A.A. Hurwitz, and J.P. Allison. 1999. Combination immunotherapy of B16 melanoma using anti-cytotoxic T lymphocyte-associated antigen 4 (CTLA-4) and granulocyte/macrophage colony-stimulating factor (GM-CSF)-producing vaccines induces rejection of subcutaneous and metastatic tumors accompanied by autoimmune depigmentation. *J. Exp. Med.* 190:355–366.
43. Rosenberg, S.A., N.P. Restifo, J.C. Yang, R.A. Morgan, and M.E. Dudley. 2008. Adoptive cell transfer: a clinical path to effective cancer immunotherapy. *Nat. Rev. Cancer.* 8:299–308.
44. Gattinoni, L., D.J. Powell Jr., S.A. Rosenberg, and N.P. Restifo. 2006. Adoptive immunotherapy for cancer: building on success. *Nat. Rev. Immunol.* 6:383–393.
45. June, C.H. 2007. Adoptive T cell therapy for cancer in the clinic. *J. Clin. Invest.* 117:1466–1476.
46. Klebanoff, C.A., L. Gattinoni, P. Torabi-Parizi, K. Kerstann, A.R. Cardones, S.E. Finkelstein, D.C. Palmer, P.A. Antony, S.T. Hwang, S.A. Rosenberg, et al. 2005. Central memory self/tumor-reactive CD8+ T cells confer superior antitumor immunity compared with effector memory T cells. *Proc. Natl. Acad. Sci. USA.* 102:9571–9576.
47. Gattinoni, L., C.A. Klebanoff, D.C. Palmer, C. Wrzesinski, K. Kerstann, Z. Yu, S.E. Finkelstein, M.R. Theoret, S.A. Rosenberg, and N.P. Restifo. 2005. Acquisition of full effector function in vitro paradoxically impairs the in vivo antitumor efficacy of adoptively transferred CD8+ T cells. *J. Clin. Invest.* 115:1616–1626.
48. Brentjens, R.J., J.B. Latouche, E. Santos, F. Marti, M.C. Gong, C. Lyddane, P.D. King, S. Larson, M. Weiss, I. Riviere, and M. Sadelain. 2003. Eradication of systemic B-cell tumors by genetically targeted human T lymphocytes co-stimulated by CD80 and interleukin-15. *Nat. Med.* 9:279–286.
49. Berger, C., M.C. Jensen, P.M. Lansdorp, M. Gough, C. Elliott, and S.R. Riddell. 2008. Adoptive transfer of effector CD8+ T cells derived from central memory cells establishes persistent T cell memory in primates. *J. Clin. Invest.* 118:294–305.
50. Schwartzentruber, D.J., S.S. Hom, R. Dadmarz, D.E. White, J.R. Yannelli, S.M. Steinberg, S.A. Rosenberg, and S.L. Topalian. 1994. In vitro predictors of therapeutic response in melanoma patients receiving tumor-infiltrating lymphocytes and interleukin-2. *J. Clin. Oncol.* 12:1475–1483.
51. Calzascia, T., F. Masson, W. Di Berardino-Besson, E. Contassot, R. Wilmotte, M. Aurrand-Lions, C. Ruegg, P.Y. Dietrich, and P.R. Walker. 2005. Homing phenotypes of tumor-specific CD8 T cells are predetermined at the tumor site by crosspresenting APCs. *Immunity.* 22:175–184.
52. Wherry, E.J., and R. Ahmed. 2004. Memory CD8 T-cell differentiation during viral infection. *J. Virol.* 78:5535–5545.
53. Foulds, K.E., and H. Shen. 2006. Clonal competition inhibits the proliferation and differentiation of adoptively transferred TCR transgenic CD4 T cells in response to infection. *J. Immunol.* 176:3037–3043.
54. Kedl, R.M., W.A. Rees, D.A. Hildeman, B. Schaefer, T. Mitchell, J. Kappler, and P. Marrack. 2000. T cells compete for access to antigen-bearing antigen-presenting cells. *J. Exp. Med.* 192:1105–1113.
55. Garcia, Z., E. Pradelli, S. Celli, H. Beuneu, A. Simon, and P. Bousso. 2007. Competition for antigen determines the stability of T cell-dendritic cell interactions during clonal expansion. *Proc. Natl. Acad. Sci. USA.* 104:4553–4558.
56. Pittet, M.J., D. Valmori, P.R. Dunbar, D.E. Speiser, D. Lienard, F. Lejeune, K. Fleischhauer, V. Cerundolo, J.C. Cerottini, and P. Romero. 1999. High frequencies of naive Melan-A/MART-1-specific CD8(+) T cells in a large proportion of human histocompatibility leukocyte antigen (HLA)-A2 individuals. *J. Exp. Med.* 190:705–715.
57. Dutoit, V., V. Rubio-Godoy, M.J. Pittet, A. Zippelius, P.Y. Dietrich, F.A. Legal, P. Guillaume, P. Romero, J.C. Cerottini, R.A. Houghten, et al. 2002. Degeneracy of antigen recognition as the molecular basis for the high frequency of naive A2/Melan-a peptide multimer(+) CD8(+) T cells in humans. *J. Exp. Med.* 196:207–216.
58. Lonchay, C., P. van der Bruggen, T. Connerotte, T. Hanagiri, P. Coulie, D. Colau, S. Lucas, A. Van Pel, K. Thielemans, N. van Baren, and T. Boon. 2004. Correlation between tumor regression and T cell responses in melanoma patients vaccinated with a MAGE antigen. *Proc. Natl. Acad. Sci. USA.* 101(Suppl 2):14631–14638.
59. Coulie, P.G., V. Karanikas, D. Colau, C. Lurquin, C. Landry, M. Marchand, T. Dorval, V. Brichard, and T. Boon. 2001. A monoclonal cytolytic T-lymphocyte response observed in a melanoma patient vaccinated with a tumor-specific antigenic peptide encoded by gene MAGE-3. *Proc. Natl. Acad. Sci. USA.* 98:10290–10295.

60. Coulie, P.G., V. Karanikas, C. Lurquin, D. Colau, T. Connerotte, T. Hanagiri, A. Van Pel, S. Lucas, D. Godelaine, C. Lonchay, et al. 2002. Cytolytic T-cell responses of cancer patients vaccinated with a MAGE antigen. *Immunol. Rev.* 188:33–42.
61. Stemberger, C., K.M. Huster, M. Koffler, F. Anderl, M. Schiemann, H. Wagner, and D.H. Busch. 2007. A single naive CD8+ T cell precursor can develop into diverse effector and memory subsets. *Immunity.* 27:985–997.
62. Chang, J.T., V.R. Palanivel, I. Kinjyo, F. Schambach, A.M. Intlekofer, A. Banerjee, S.A. Longworth, K.E. Vinup, P. Mrass, J. Oliaro, et al. 2007. Asymmetric T lymphocyte division in the initiation of adaptive immune responses. *Science.* 315:1687–1691.
63. Catron, D.M., L.K. Rusch, J. Hataye, A.A. Itano, and M.K. Jenkins. 2006. CD4+ T cells that enter the draining lymph nodes after antigen injection participate in the primary response and become central-memory cells. *J. Exp. Med.* 203:1045–1054.
64. Kedl, R.M., J.W. Kappler, and P. Marrack. 2003. Epitope dominance, competition and T cell affinity maturation. *Curr. Opin. Immunol.* 15:120–127.
65. Ferrone, C.R., M.A. Perales, S.M. Goldberg, C.J. Somberg, D. Hirschhorn-Cymerman, P.D. Gregor, M.J. Turk, T. Ramirez-Montagut, J.S. Gold, A.N. Houghton, and J.D. Wolchok. 2006. Adjuvanticity of plasmid DNA encoding cytokines fused to immunoglobulin Fc domains. *Clin. Cancer Res.* 12:5511–5519.
66. Seder, R.A., P.A. Darrah, and M. Roederer. 2008. T-cell quality in memory and protection: implications for vaccine design. *Nat. Rev. Immunol.* 8:247–258.
67. Makedonas, G., and M.R. Betts. 2006. Polyfunctional analysis of human T cell responses: importance in vaccine immunogenicity and natural infection. *Springer Semin. Immunopathol.* 28:209–219.
68. Rifa'I, M., Y. Kawamoto, I. Nakashima, and H. Suzuki. 2004. Essential roles of CD8+CD122+ regulatory T cells in the maintenance of T cell homeostasis. *J. Exp. Med.* 200:1123–1134.
69. Endharti, A.T., M. Rifa'I, Z. Shi, Y. Fukuoka, Y. Nakahara, Y. Kawamoto, K. Takeda, K. Isobe, and H. Suzuki. 2005. Cutting edge: CD8+CD122+ regulatory T cells produce IL-10 to suppress IFN-gamma production and proliferation of CD8+ T cells. *J. Immunol.* 175:7093–7097.
70. Dudley, M.E., J.R. Wunderlich, P.F. Robbins, J.C. Yang, P. Hwu, D.J. Schwartzentruber, S.L. Topalian, R. Sherry, N.P. Restifo, A.M. Hubicki, et al. 2002. Cancer regression and autoimmunity in patients after clonal repopulation with antitumor lymphocytes. *Science.* 298:850–854.
71. Morgan, R.A., M.E. Dudley, J.R. Wunderlich, M.S. Hughes, J.C. Yang, R.M. Sherry, R.E. Royal, S.L. Topalian, U.S. Kammula, N.P. Restifo, et al. 2006. Cancer regression in patients after transfer of genetically engineered lymphocytes. *Science.* 314:126–129.
72. Powell, D.J. Jr., M.E. Dudley, K.A. Hogan, J.R. Wunderlich, and S.A. Rosenberg. 2006. Adoptive transfer of vaccine-induced peripheral blood mononuclear cells to patients with metastatic melanoma following lymphodepletion. *J. Immunol.* 177:6527–6539.
73. Dudley, M.E., J.R. Wunderlich, J.C. Yang, R.M. Sherry, S.L. Topalian, N.P. Restifo, R.E. Royal, U. Kammula, D.E. White, S.A. Mavroukakis, et al. 2005. Adoptive cell transfer therapy following non-myeloablative but lymphodepleting chemotherapy for the treatment of patients with refractory metastatic melanoma. *J. Clin. Oncol.* 23:2346–2357.
74. Yee, C., J.A. Thompson, D. Byrd, S.R. Riddell, P. Roche, E. Celis, and P.D. Greenberg. 2002. Adoptive T cell therapy using antigen-specific CD8+ T cell clones for the treatment of patients with metastatic melanoma: in vivo persistence, migration, and antitumor effect of transferred T cells. *Proc. Natl. Acad. Sci. USA.* 99:16168–16173.
75. Naldini, L., U. Blomer, P. Gallay, D. Ory, R. Mulligan, F.H. Gage, I.M. Verma, and D. Trono. 1996. In vivo gene delivery and stable transduction of nondividing cells by a lentiviral vector. *Science.* 272:263–267.
76. Trowbridge, I.S., and C. Mazauskas. 1976. Immunological properties of murine thymus-dependent lymphocyte surface glycoproteins. *Eur. J. Immunol.* 6:557–562.
77. Turk, M.J., J.A. Guevara-Patino, G.A. Rizzuto, M.E. Engelhorn, S. Sakaguchi, and A.N. Houghton. 2004. Concomitant tumor immunity to a poorly immunogenic melanoma is prevented by regulatory T cells. *J. Exp. Med.* 200:771–782.
78. Savage, P.A., K. Vosseller, C. Kang, K. Larimore, E. Riedel, K. Wojnoonski, A.A. Jungbluth, and J.P. Allison. 2008. Recognition of a ubiquitous self antigen by prostate cancer-infiltrating CD8+ T lymphocytes. *Science.* 319:215–220.
79. Lefranc, M.P., V. Giudicelli, Q. Kaas, E. Duprat, J. Jabado-Michaloud, D. Scaviner, C. Ginestoux, O. Clement, D. Chaume, and G. Lefranc. 2005. IMGT, the international ImMunoGeneTics information system. *Nucleic Acids Res.* 33:D593–D597.
80. Lamoreaux, L., M. Roederer, and R. Koup. 2006. Intracellular cytokine optimization and standard operating procedure. *Nat. Protoc.* 1:1507–1516.